AD-A120 768 AB INITIO INFRARED AND RAMAN SPECTRA(U) CALIFORNIA UNIV 1/1
SAN DIEGO LA JOLLA DEPT OF PHYSICS D R FREDKIN ET AL.
AUG 82 TR-9 N00014-78-C-0325

UNCLASSIFIED F/G 7/4 NL

END

FILMED

DTIC

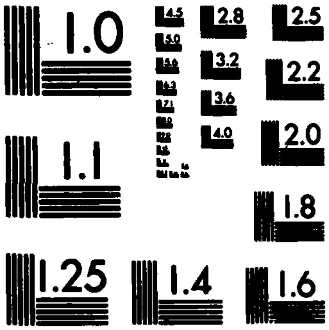
1.0
1.1
1.25
1.4
1.6
1.8
2.0
2.2
2.5
2.8
3.2
3.6
4.0
4.5
5.0
5.6
6.3
7.1

MICROCOPY RESOLUTION TEST CHART
NATIONAL BUREAU OF STANDARDS-1963-A

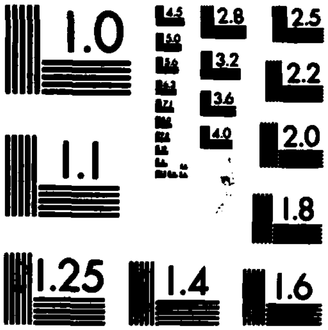
1.0
1.1
1.25
1.4
1.6
1.8
2.0
2.2
2.5
2.8
3.2
3.6
4.0
4.5
5.0
5.6
6.3
7.1

MICROCOPY RESOLUTION TEST CHART
NATIONAL BUREAU OF STANDARDS-1963-A

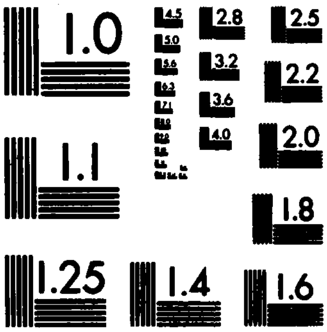
1.0
1.1
1.25
1.4
1.6
1.8
2.0
2.2
2.5
2.8
3.2
3.6
4.0
4.5
5.0
5.6
6.3
7.1

MICROCOPY RESOLUTION TEST CHART
NATIONAL BUREAU OF STANDARDS-1963-A

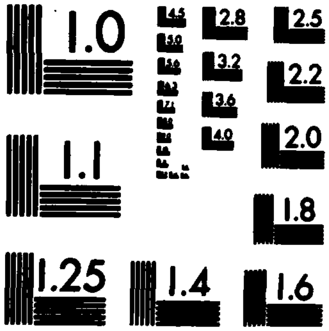
1.0
1.1
1.25
1.4
1.6
1.8
2.0
2.2
2.5
2.8
3.2
3.6
4.0
4.5
5.0
5.6
6.3
7.1

MICROCOPY RESOLUTION TEST CHART
NATIONAL BUREAU OF STANDARDS-1963-A

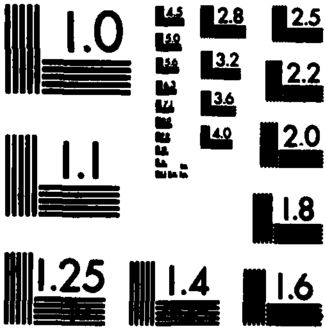
1.0
1.1
1.25
1.4
1.6
1.8
2.0
2.2
2.5
2.8
3.2
3.6
4.0
4.5
5.0
5.6
6.3
7.1

MICROCOPY RESOLUTION TEST CHART
NATIONAL BUREAU OF STANDARDC-1963-A

AD A120768

DTIC FILE COPY

SECURITY CLASSIFICATION OF THIS PAGE (When Data Entered)

REPORT DOCUMENTATION PAGE

READ INSTRUCTIONS BEFORE COMPLETING FORM

1. REPORT NUMBER
9 ④

2. GOVT ACCESSION NO.
AD A12076 ✓

3. RECIPIENT'S CATALOG NUMBER

4. TITLE (and Subtitle)
AB INITIO INFRARED AND RAMAN SPECTRA

5. TYPE OF REPORT & PERIOD COVERED
Technical Report

6. PERFORMING ORG. REPORT NUMBER

7. AUTHOR(s)
Donald R. Fredkin, Andrew Komornicki,
Steven R. White and Kent R. Wilson

8. CONTRACT OR GRANT NUMBER(s)
ONR N00014-78 C-0325

9. PERFORMING ORGANIZATION NAME AND ADDRESS
University of California, San Diego
La Jolla, California 92093

10. PROGRAM ELEMENT, PROJECT, TASK AREA & WORK UNIT NUMBERS

11. CONTROLLING OFFICE NAME AND ADDRESS
Office of Naval Research
Arlington, VA 22217

12. REPORT DATE
August, 1982

13. NUMBER OF PAGES
25

14. MONITORING AGENCY NAME & ADDRESS(if different from Controlling Office)

15. SECURITY CLASS. (of this report)
Unclassified

15a. DECLASSIFICATION/DOWNGRADING SCHEDULE

16. DISTRIBUTION STATEMENT (of this Report)
This document has been approved for public release and sale; its distribution is unlimited.

17. DISTRIBUTION STATEMENT (of the abstract entered in Block 20, if different from Report)

DTIC
SELECTE
OCT 27 1982
S
H
D

18. SUPPLEMENTARY NOTES
Submitted for publication to the Journal of Chemical Physics

19. KEY WORDS (Continue on reverse side if necessary and identify by block number)
infrared spectra
Raman spectra
molecular absorption
electronic absorption
molecular dynamics

20. ABSTRACT (Continue on reverse side if necessary and identify by block number)

We discuss several ways in which molecular absorption and scattering spectra can be computed *ab initio*, from the fundamental constants of nature. These methods can be divided into two general categories. In the first, or *sequential*, type of approach, one first solves the electronic part of the Schrödinger equation in the Born-Oppenheimer approximation, mapping out the potential energy, dipole moment vector (for infrared absorption) and polarizability tensor (for Raman scattering) as functions of nuclear coordinates. Hav-

DD FORM 1 JAN 73 1473 EDITION OF 1 NOV 65 IS OBSOLETE
S/N 0102-LF-014-6601

SECURITY CLASSIFICATION OF THIS PAGE (When Data Entered)

Block 20. Abstract (continued from front page)

ing completed the electronic part of the calculation, one then solves the nuclear part of the problem either classically or quantum mechanically. As an example of the *sequential ab initio* approach, the infrared and Raman rotational and vibrational-rotational spectral band contours for the water molecule are computed in the simplest rigid rotor, normal mode approximation. Quantum techniques, are used to calculate the necessary potential energy, dipole moment, and polarizability information at the equilibrium geometry. A new quick, accurate, and easy to program classical technique involving no reference to Euler angles or special functions is developed to compute the infrared and Raman band contours for any rigid rotor, including asymmetric tops. A second, or *simultaneous*, type of *ab initio* approach is suggested for large systems, particularly those for which normal mode analysis is inappropriate, such as liquids, clusters, or floppy molecules. ~~Then the curse of dimensionality prevents map~~ping out in advance the complete potential, dipole moment, and polarizability functions over the whole space of nuclear positions of all atoms, and a solution in which the electronic and nuclear parts of the Born-Oppenheimer approximation are simultaneously solved is needed. A quantum force classical trajectory (QFCT) molecular dynamic method, based on linear response theory, is described, in which the forces, dipole moment, and polarizability are computed quantum mechanically, using gradient techniques step by step along a classical trajectory whose path is determined by these quantum forces. We believe the QFCT method to be a more practical *ab initio* route to spectral band contours for large molecules, clusters, and solutions, and it can be equally applied to equilibrium and non-equilibrium systems. It is pointed out that a similar *ab initio* QFCT molecular dynamic approach could be used to compute other types of spectra, for example electronic absorption, as well as other parameters such as transport properties and thermodynamic functions and their quantum corrections. For parameters not depending on momenta, a parallel *ab initio* Monte Carlo approach would use electronic energies and other parameters of interest generated quantum mechanically, and "classical" trial moves of the nuclei.

DTIC
COPY
INSPECTED
2

Accession For
NTIS GRA&I ☑
DTIC TAB ☐
Unannounced ☐
Justification

By
Distribution/
Availability Codes
Dist | Avail and/or Special
A

OFFICE OF NAVAL RESEARCH

Contract N00014-78 C-0325

TECHNICAL REPORT NO. 9

AB INITIO INFRARED AND RAMAN SPECTRA

BY

Donald R. Fredkin
Department of Physics
University of California, San Diego
La Jolla, CA 92093

Andrew Komornicki
Polyatomics Research Institute
Mountain View, CA 94043

AND

Steven R. White and Kent R. Wilson
Department of Chemistry
University of California, San Diego
La Jolla, CA 92093

Prepared for Publication
in
The Journal of Chemical Physics

Reproduction in whole or in part is permitted for any purpose ie United States Government.

This document has been approved for public release and sale; its distribution is unlimited.

AB INITIO INFRARED AND RAMAN SPECTRA

Donald R. Fredkin

Department of Physics
University of California, San Diego
La Jolla, CA 92093

*Andrew Komornicki**

Polyatomics Research Institute
Mountain View, CA 94043

Steven R. White† *and Kent R. Wilson*

Department of Chemistry
University of California, San Diego
La Jolla, CA 92093

ABSTRACT

We discuss several ways in which molecular absorption and scattering spectra can be computed *ab initio*, from the fundamental constants of nature. These methods can be divided into two general categories. In the first, or *sequential*, type of approach, one first solves the electronic part of the Schrödinger equation in the Born-Oppenheimer approximation, mapping out the potential energy, dipole moment vector (for infrared absorption) and polarizability tensor (for Raman scattering) as functions of nuclear coordinates. Having completed the electronic part of the calculation, one then solves the nuclear part of the problem either classically or quantum mechanically. As an example of the *sequential ab initio* approach, the infrared and Raman rotational and vibrational-rotational spectral band contours for the water molecule are computed in the simplest rigid rotor, normal mode approximation. Quantum techniques, are used to calculate the necessary potential energy, dipole moment, and polarizability information at the equilibrium geometry. A new quick, accurate, and easy to program classical technique involving no reference to Euler angles or special functions is developed to compute the infrared and Raman band contours for any rigid rotor, including asymmetric tops. A second, or *simultaneous*, type of *ab initio* approach is suggested for large systems, particularly those for which normal mode analysis is inappropriate, such as liquids, clusters, or floppy molecules. Then the curse of dimensionality prevents mapping out in advance the complete potential, dipole moment, and polarizability functions over the whole space of nuclear positions of all atoms, and a solution in which the electronic and nuclear parts of the Born-Oppenheimer approximation are simultaneously solved is needed. A quantum force classical trajectory (QFCT) molecular dynamic method, based on linear response theory, is described, in which the forces, dipole moment, and polarizability are computed quantum mechanically, using gradient techniques step by step along a classical trajectory whose path is determined by these quantum forces. We believe the QFCT method to be a more practical *ab initio* route to spectral band contours for large molecules, clusters, and solutions, and it can be equally applied to equilibrium and non-equilibrium systems. It is pointed out that a similar *ab initio* QFCT molecular dynamic approach could be used to compute other types of spectra, for example electronic absorption, as well as other parameters such as transport properties and thermodynamic functions and their quantum corrections. For parameters not depending on momenta, a parallel *ab initio* Monte Carlo approach would use electronic energies and other parameters of interest generated quantum mechanically, and "classical" trial moves of the nuclei.

Submitted to *J. Chem. Phys.* August 1982

[*] Address: 1101 San Antonio Rd., Suite 420
[†] Present address: Dept. of Physics, Cornell University, Ithaca, N.Y. 14853

PACS numbers: 33.10.Cs, 33.10.Jz, 33.70.Jg, 31.20.Di

AB INITIO INFRARED AND RAMAN SPECTRA

Donald R. Fredkin

Department of Physics
University of California, San Diego
La Jolla, CA 92093

Andrew Komornicki[*]

Polyatomics Research Institute
Mountain View, CA 94043

Steven R. White[†] *and Kent R. Wilson*

Department of Chemistry
University of California, San Diego
La Jolla, CA 92093

I. INTRODUCTION

With increased computer power and improved computational techniques, such as the gradient methods described in Sections III and IV below, it is becoming practical to compute spectra *ab initio*, from the fundamental constants of nature, for systems of increasing complexity. Such an approach is appealing not only because of the usual academic desire to elegantly derive observed phenomena from first principles, but also because of the practical desire to be able to experimentally identify and understand transient species or states (such as those existing during the course of chemical reactions) whose spectral properties cannot be deduced from equilibrium measurements. Therefore in this paper we explore several possible *ab initio* approaches to spectra, specifically focusing on infrared and nonresonance Raman. Many of the points discussed can, however, also be extended to other types of spectra such as electronic absorption and resonance Raman.

We discuss two approaches, *sequential* and *simultaneous*. The *sequential* approach, in which first the electronic part and then later the nuclear part of the Born-Oppenheimer approximation is solved, is appropriate for small systems. The *simultaneous* approach, in which the electronic and nuclear parts are solved at the same time, is more appropriate for many atom systems. Then we review the newer quantum gradient techniques which greatly simplify *ab initio* calculations of spectra. As a simple illustration of a *sequential ab initio* calculation, we compute the infrared and Raman spectral band contours for the water molecule using a rigid rotor, normal mode approach. The vibrations are handled quantum mechanically, but in order to make the connection to liquid state spectra in which the individual rovibrational lines have usually merged, we compute here the band contours. While this could be done, as illustrated elsewhere,[1,2] by broadening the quantum rovibrational lines,[3,4] we choose instead in this paper to explore another path, computing the band contours classically in the rigid rotor limit, with the aim of eventually gaining a more intuitive understanding of the relation among moments of inertia, dipole and polarizability derivatives, temperature, and band contour shape. The classical technique we have developed is a simple, quick, and easy way to compute band contours, and might be used, for example, to conveniently explore the dipole and polarizability components consistent with measured spectra. Once the rotational correlation functions have been

---

The authors provided phototypeset copy for this paper using REFER | TBL | EQN | TROFF on UNIX.

computed from the moments of inertia and Fourier transformed, one could compute band contours immediately for any combination of dipole and polarizability derivatives simply by weighting these transformed correlation functions by the appropriate dipole or polarizability components and summing. An on-line visual matching of theoretical to experimental infrared and Raman band contours is quite possible and might be very instructive in understanding the physical basis of observed spectra, for example the symmetries and directions of dipole moment and polarizability changes associated with different vibrations. This can be carried out even in the absence of potential energy surface information of sufficient accuracy to match line spectra. In this way, for example, one could use crude *ab initio* dipole and polarizability parameters to help resolve the usual experimental sign uncertainties and then refine the parameters by more detailed comparison with experimental band contours. We derive the appropriate equations to compute infrared and Raman spectra and present our *ab initio sequential* rigid rotor, normal mode band contour results for H_2O and compare with experiment. Finally we describe in more detail our proposed *ab initio simultaneous* approach, which can in principle allow the computation of spectra and many other properties for larger systems using a close linking of quantum evaluation of forces and other parameters with classical trajectory integration.

II. SEQUENTIAL VERSUS SIMULTANEOUS APPROACHES

In the usual *sequential* approach, the electronic part of the Born-Oppenheimer approximation is first solved for the potential energy V as a function of the positions of the nuclei, and for the connection to the radiation field, for example the dipole moment vector $\boldsymbol{\mu}$ for infrared spectra and the polarizability tensor $\mathbf{P}$ for Raman spectra. The least complicated *sequential ab initio* approach, which we illustrate here by a calculation of the infrared and Raman spectral band contours for the water molecule, is to search for the minimum of the potential energy surface and then to expand V, $\boldsymbol{\mu}$, and $\mathbf{P}$ in Taylor's series about this minimum. At the simplest level, a rigid rotor, normal mode approximation can be made for the nuclear rotational - vibrational (rovibrational) wavefunctions and the derivatives of $\boldsymbol{\mu}$ and $\mathbf{P}$ with respect to the normal coordinates can then be used to compute the intensities of the various rovibrational transitions.[1,2,5,6] Higher derivatives in the Taylor's series for V, $\boldsymbol{\mu}$, and $\mathbf{P}$ can be used in more accurate calculations. An even more accurate *sequential* solution, applicable if the molecule is quite small, is to solve for V, $\boldsymbol{\mu}$, and $\mathbf{P}$ over all the necessary coordinate space and then numerically to solve for the rovibrational eigenfunctions and energy eigenvalues, and finally numerically to solve for the transition intensities. An interesting and instructive discussion of various theoretical approaches to the computation of infrared spectra with particular application to water monomers, dimers, and liquid water has recently been given by Coker, Reimers, and Watts.[7] An intriguing *ab initio* calculation for the N_2 molecule has been carried out by Svendsen and Oddershede[8] who use the frequency dependent polarizability tensor instead of the usual static one. Several other types of semiclassical *sequential* approaches could also be carried out in an *ab initio* fashion.[9,10]

For molecular systems of more than a few atoms, the *simultaneous* approach to *ab initio* calculations is preferred. As the size of the system increases, it becomes increasingly impractical to link quantum mechanics to experimental observables through the complete multidimensional computation and storage of intermediate functions of nuclear coordinates such as potential energy V, dipole moment $\boldsymbol{\mu}$, and polarizability $\mathbf{P}$. As the number N of atoms grows, the "curse of dimensionality" makes the explicit computation as well as the fitting and storage of such functions infeasible. For example, if 10 grid points are needed for sufficient accuracy in each dimension, then 10^{3N} evaluations are needed to specify the full function, or 10^{36} if a dozen atoms are involved. Clearly, no experimental measurement contains or can require this much information, and a different theoretical approach is called for. An alternative is statistical sampling, for example using a molecular dynamics or Monte Carlo approach. Specifically, as one of us has suggested,[11] classical molecular dynamics may be integrated with *ab initio* quantum force evaluation, so that at each time step the force on each nucleus is evaluated quantum mechanically and then used to integrate forward one step at a time the classical trajectory. One would follow the trajectory in time, sampling the force $\mathbf{F}_i = -\frac{\partial V}{\partial \mathbf{r}_i}$, the dipole moment $\boldsymbol{\mu}$, and the polarizability P only at specific nuclear configurations through which the trajectory passes, and then apply the techniques illustrated in previous papers[1,2] to derive the infrared and Raman spectra from the power spectra of the time histories of $\mu(t)$ and $P(t)$. While this sampling may build up over the course of many trajectories a continuously improving estimate of the entire V, μ and P functions over the accessible volume of configuration space, we do not initially require a global representation of the functions, and in systems of many atoms we are likely to achieve sufficient accuracy to compare with experiment long before such a global representation could be computed. With an average over the proper ensemble of initial nuclear positions and momenta, observables ranging from thermodynamic functions to spectra to chemical reaction properties to transport properties could be computed in this way. An alternative approach, for phenomena which are not explicitly time dependent, is a Monte Carlo procedure in which at each trial nuclear configuration step the energy is evaluated quantum mechanically, and for accepted steps the other variables of interest are then computed.

Two initial calculations of this type, which for the molecular dynamics case we will call Quantum Force Classical Trajectory (QFCT), have been carried out by Warshel and Karplus[12] and by Leforestier.[13] Warshel and Karplus[12] use forces given from analytical first derivatives in a semiclassical technique to integrate the equations of motion for *cis-trans* photoisomerization from the triplet state of butene-2. Leforestier[13] studied the gas phase nucleophilic substitution reaction $H^- + CH_4 \rightarrow CH_4 + H^-$. He derived his forces using an *ab initio* approach which will be reviewed below and integrated the classical trajectories outward from an initial state corresponding to the transition state for the reaction.

Thus, classical statistical mechanics plus an *ab initio* QFCT method can be used to predict spectral observables, computing the time evolution of the dipole moment vector $\mu(t)$ and the polarizability tensor $P(t)$, and, as we have previously demonstrated, from ensemble averages of their power spectra the infrared[1] and Raman[2] spectra. This can be extended to computing infrared and Raman spectra for more complex systems, such as clusters and liquid solutions, and transient spectra during chemical reactions,[14] or in other words to situations for which only band contours may be observable experimentally and for which trying to quantize nuclear motion would be too difficult theoretically. We emphasize i) that other spectral and transport phenomena could also similarly be derived through calculation of their proper correlation functions,[15-18] ii) that thermodynamic variables and their quantum corrections could be computed,[19] and iii) that the parallel Monte Carlo approach for properties independent of momenta would be quantum evaluation of energy (plus force[20-22] if desired) at each trial step followed by evaluation of other variables to be averaged for those configurations which are accepted.

III. QUANTUM POTENTIAL ENERGY, FORCE, AND EQUILIBRIUM GEOMETRY

The emergence of gradient methods in recent years allows the use of very efficient methods for the calculation of forces, the location of equilibrium structures and the evaluation of harmonic force constants and vibrational frequencies.[23-30] More recently, one of us has suggested that the power of these methods also be used to evaluate the dipole and polarizability derivatives.[31,32] (For an example of infrared vibrational properties computed without gradient techniques see Person, Brown, Steele, and Peters.[33,34]) In Sections III and IV we summarize the salient points of the gradient approach and show how these methods are used to evaluate the relevant quantities required in the example *sequential ab initio* spectral analysis for the H_2O infrared and Raman band contours presented below. The molecular calculations reported here are all performed at the SCF level with the GRADSCF program system.[35]

In many chemical applications one needs to evaluate a molecular wavefunction from which the energy, dipole moment and other relevant properties are calculated. It was recognized a number of years ago[36-39] that often a knowledge not only of the energy U, but also of its first derivatives with respect to the nuclear coordinates can considerably enhance the scope of chemical computational investigations. Over the past decade efficient means of evaluating the first derivatives of the energy have been developed, first for semiempirical[24] and eventually for *ab initio* wavefunctions.[23,28,40] In these applications both the energy and the gradient are evaluated simultaneously. The derivation of the gradient expression for a variety of wavefunctions has been extensively discussed in the literature[23,28,40] and will not be repeated here.

If we expand the energy as a function of the nuclear coordinates in a Taylor's series we find that

$$U(X) = U(X_0) + g^{\dagger}(X - X_0) + (X - X_0)^{\dagger}Q(X - X_0) \tag{3.1}$$

where X is the vector of Cartesian nuclear coordinates, g is the gradient vector whose elements are defined as $g_i = \frac{\partial U}{\partial X_i}$, and Q is the Hessian, or matrix of second derivatives. The geometry optimization is performed by employing the following algorithm,

$$X = X_0 - \alpha Q^{-1} g\,, \tag{3.2}$$

where α is a scale factor. The specific minimization algorithm which we use is that of Murtaugh and Sargent [41] where the matrix Q is initially approximated by a unit matrix and updated after each successive step to form the inverse to the true Hessian. Convergence in the geometry optimization is deemed satisfactory if the largest component of the gradient is less than 4×10^{-4} hartree/bohr.

The force constants are evaluated by the finite difference techniques described previously.[25-27] By numerically differencing the gradient vector we are able to evaluate a column of the matrix of second derivatives for each displacement of the nuclear coordinates. The force constants are evaluated in a Cartesian representation and the frequencies and normal modes are determined by diagonalizing the mass weighted force constant matrix.[5,25-27] We also evaluate the appropriate B matrix[5,6,28] which in turn is used to transform the force constants from a Cartesian to an internal symmetry coordinate representation. This transformation serves rigorously to project out any translation and rotation from the vibrational modes and yields six true zero frequency modes.

The water molecule results for the equilibrium geometry, moments of inertia, and vibrational frequencies derived from harmonic force constants are shown in Table I. Here r is the O-H distance, θ is the H-O-H angle, $I_{\alpha\alpha}$ is the $\alpha\alpha$ component of the moment of inertia tensor, Å is Angstrom, deg is degrees, amu is atomic mass units, and cm^{-1} is wavenumbers in inverse centimeters. Figure 1 shows the Cartesian axis system chosen for the water molecule,[42] and Fig. 2 shows the normal modes.[42] The symmetric stretch corresponds to ν_1 and q_1, ν_2 and q_2 correspond to the symmetric bend, and ν_3 and q_3 correspond to the asymmetric stretch, in which ν_i denotes the ith normal mode frequency and q_i is the ith normal coordinate.

TABLE I. *Ab initio* parameters computed for H_2O molecule.

r (Å)	θ (deg)	I_{xx} (*amu* Å^2)	I_{yy} (*amu* Å^2)	I_{zz} (*amu* Å^2)	ν_1 (cm^{-1})	ν_2 (cm^{-1})	ν_3 (cm^{-1})
0.943	106.0	1.720	0.5766	1.1434	3797	1740	3902

IV. QUANTUM DIPOLE MOMENT AND POLARIZABILITY TENSOR

The dipole and polarizability derivatives with respect to the normal modes are computed using a very efficient new method which has been reported previously.[31,32] We seek for the infrared spectrum the quantities

$$\frac{\partial \mu_\alpha}{\partial q_j} \tag{4.1}$$

where μ_α, α = x,y,z, are the three components of the molecule fixed dipole moment vector μ and the q_j are the normal mode coordinates. For the polarizability derivatives we seek the analogous quantities

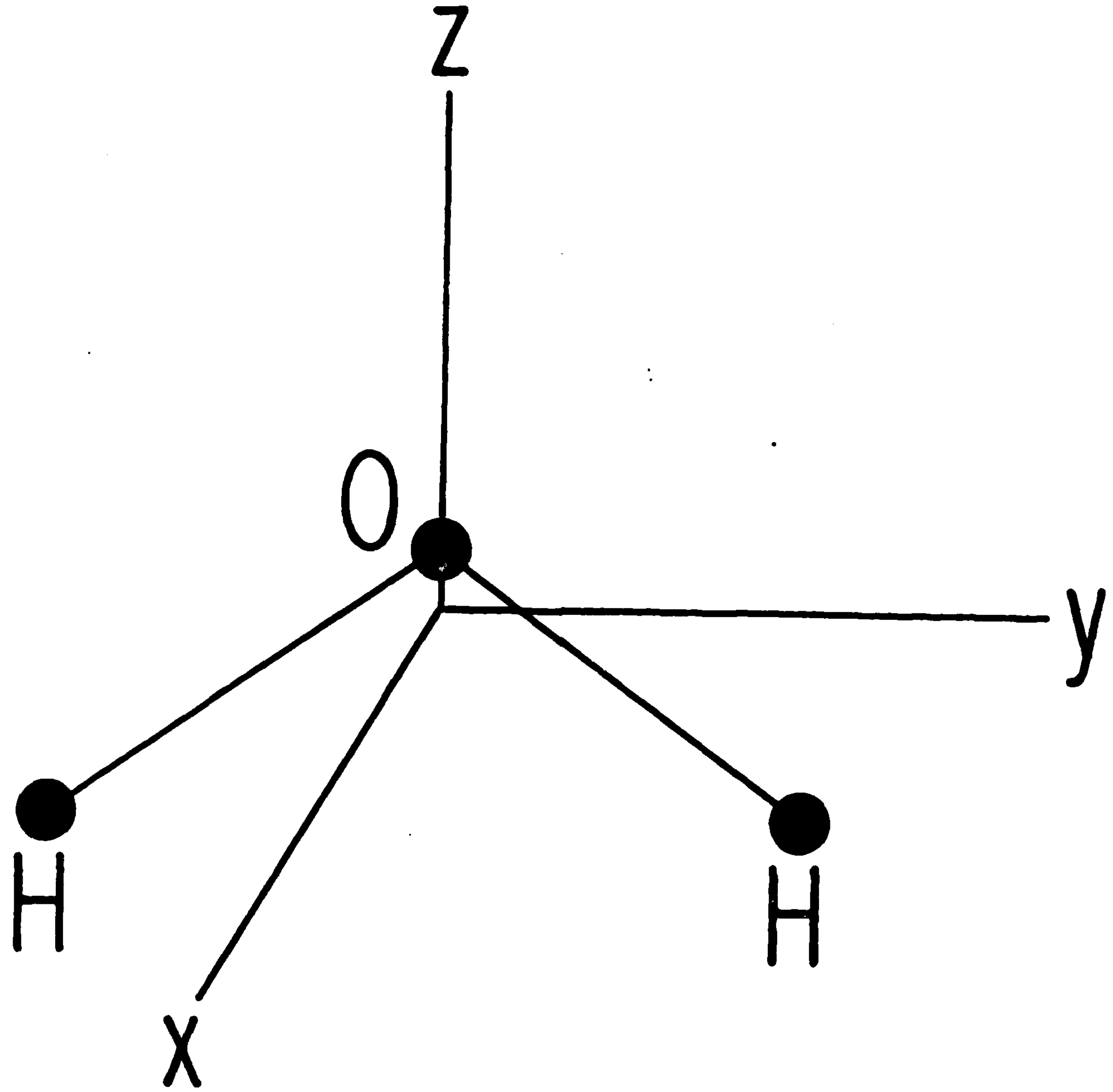

Figure 1. Body fixed axes chosen for the H_2O molecule. The yz plane is the molecular plane.

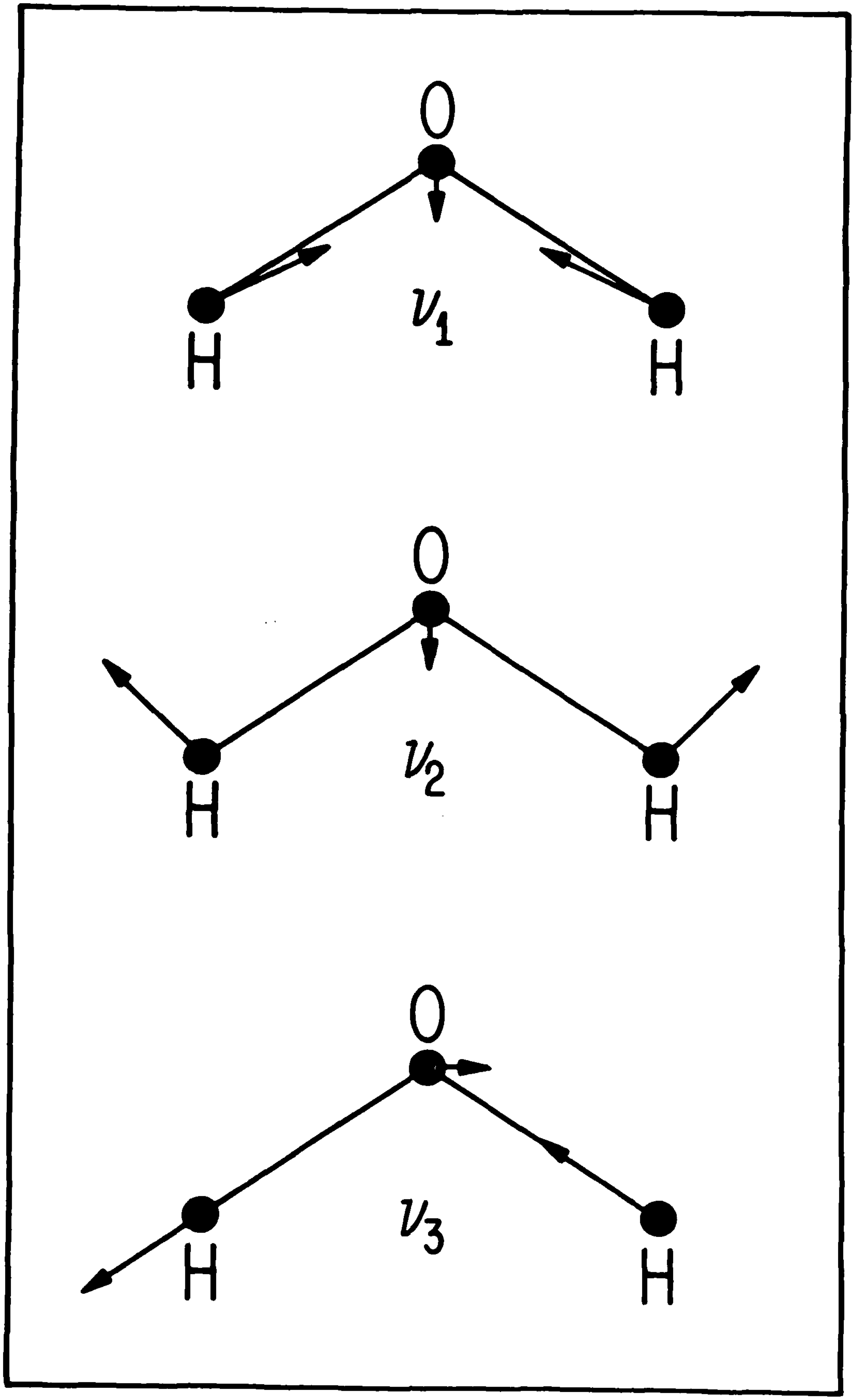
O
H
ν_1
H
O
H
ν_2
H
O
H
ν_3
H

Figure 2. Normal modes of H_2O. For clarity, the magnitudes of the oxygen motions relative to those of hydrogen have been exaggerated.

$$\frac{\partial P_{\alpha\beta}}{\partial q_j} \tag{4.2}$$

where the $P_{\alpha\beta}$ are the components of the molecule fixed polarizability tensor, in which α and $\beta = x,y,z$ and again the q_j are the normal coordinates. The dipole moment vector and the polarizability tensor are the first and second derivatives of the energy U(E) in the presence of an applied external electric field E. We can therefore write the derivatives of the elements of the dipole moment vector and polarizability tensor with respect to the Cartesian components X_i of the positions of the nuclei in the following manner, in which as before $g_i = \frac{\partial U}{\partial X_i}$,

$$\frac{\partial \mu_\alpha}{\partial X_i} = -\frac{\partial}{\partial X_i}\frac{\partial U(E)}{\partial E_\alpha} = -\frac{\partial}{\partial E_\alpha}\frac{\partial U(E)}{\partial X_i} = -\frac{\partial}{\partial E_\alpha} g_i(E) \tag{4.3}$$

and

$$\frac{\partial P_{\alpha\beta}}{\partial X_i} = -\frac{\partial}{\partial X_i}\frac{\partial^2 U(E)}{\partial E_\alpha \partial E_\beta} = -\frac{\partial^2}{\partial E_\alpha \partial E_\beta}\frac{\partial U(E)}{\partial X_i} = -\frac{\partial^2}{\partial E_\alpha \partial E_\beta} g_i(E) \tag{4.4}$$

The final terms in both equations result from the interchange in the order of differentiation. These final expressions involve the derivatives of the gradient of the energy with respect to the components of an applied electric field. If we now transform the resulting gradient vector from a Cartesian to a normal coordinate representation we arrive at the desired quantities shown in Eqs. (4.1) and (4.2). The simplicity and efficiency of the method lies in the fact that the introduction of the electric field involves only a one electron perturbation to the molecular Hamiltonian. We write the Hamiltonian as

$$H(E) = H_0 + H'(E) \tag{4.5}$$

where

$$H'(E) = e\sum_{i=1}^{elec} E\cdot r_i - e\sum_{j=1}^{nuclei} Z_j\, E\cdot R_j \tag{4.6}$$

in which e is the magnitude of the electron charge, E is the applied electric field, r_i is the position of the ith electron, the first sum is over the electrons, Z_j is the charge of the jth nucleus, R_j is its position, and the second sum is over the nuclei. For the computation of the energy this Hamiltonian requires the addition of a term which includes the appropriate dipole moment integrals. It is important to realize that the variation of the field is independent of the nuclear coordinates. In all of our calculations for the water molecule presented here the molecule is held fixed at the equilibrium geometry and SCF calculations are performed for a set of applied electric fields. For any polyatomic system, the dipole derivatives require at most six SCF calculations: two variations of the applied field in each of the three Cartesian directions. The polarizability derivatives require a total of 12 SCF calculations, since these require a two dimensional difference formula for the finite difference equations. All of these calculations use the same set of one and two electron integrals. Furthermore, the evaluation of the gradient is performed only once. In the absence of an applied field the gradient calculation yields one vector. Once we apply the field in all of the required directions, the gradient calculation yields either six or twelve vectors.

These gradient vectors, which are now a function of the electric field, are then transformed from a Cartesian to a normal coordinate representation. The resulting values are numerically differentiated to yield the dipole and polarizability derivatives.

In the geometry and force constant calculations for the water molecule we use a split-valence polarized basis which was originally developed by Pople and co-workers.[43] This basis set is described as a (10s4p1d/3s1p) contracted to a [3s2p1d/2s1p] basis and often referred to as a 6-31G** basis. The geometries and vibrational frequencies calculated with this basis are close to the limit attainable at the SCF level. The d-type polarization functions on the oxygen atom have an exponent of 0.8, while the p-type polarization functions on the hydrogen atoms are given exponents of 1.1.

The calculation of the water dipole and polarizability derivatives requires a much more extensive basis set. It has previously been shown that a large and flexible basis set is needed to describe accurately the interaction of a molecule with an applied electric field. To this end we employ a triple-zeta plus double polarization basis (TZPP) for the dipole and polarizability derivatives. This basis set provides a near Hartree-Fock description of the molecular bonding, plus a set of diffuse functions of sufficient flexibility to interact with the applied field. In these calculations we employ a Huzinaga basis of (11s6p/5s) as contracted by Dunning[44] to a [5s3p/3s] basis on the oxygen and the hydrogen atoms. This basis is augmented by two sets of d functions on the oxygen with exponents of 0.8 and 0.078, and two sets of p-type polarization functions on the hydrogens with exponents of 1.1 and 0.116. The magnitude of the applied field is chosen to be 1.0×10^{-3} au. The results of the calculation are presented in Tables II and III, in which μ_α is the α component of the dipole moment vector, $P_{\alpha\alpha}$ is the $\alpha\alpha$ diagonal element of the polarizability tensor P, D is debye, and Å is angstrom. Extensive comparison with experimentally derived values of these parameters will not be presented in this paper, and we only briefly note here that the dipole parameters may be compared with the experimental values of Camy-Peyret and Flaud[45] and the polarizability parameters with the work of Murphy.[46-48]

TABLE II. Non-zero *ab initio* equilibrium dipole moment and polarizability components.

μ_z (D)	P_{xx} (Å^3)	P_{yy} (Å^3)	P_{zz} (Å^3)
-2.02	1.0566	1.2845	1.1702

TABLE III. *Ab initio* dipole and polarizability derivatives.

	$\frac{\partial}{\partial q_1}$			$\frac{\partial}{\partial q_2}$			$\frac{\partial}{\partial q_3}$		
		(D Å^{-1} $amu^{-\frac{1}{2}}$)			(D Å^{-1} $amu^{-\frac{1}{2}}$)			(D Å^{-1} $amu^{-\frac{1}{2}}$)	
μ_x		0.0			0.0			0.0	
μ_y		0.0			0.0			1.4663	
μ_z		0.5538			1.5355			0.0	
		(Å^2$amu^{-\frac{1}{2}}$)			(Å^2$amu^{-\frac{1}{2}}$)			(Å^2$amu^{-\frac{1}{2}}$)	
	0.40349	0.0	0.0	0.0252	0.0	0.0	0.0	0.0	0.0
P	0.0	2.03936	0.0	0.0	0.18969	0.0	0.0	0.0	1.1048
	0.0	0.0	1.3186	0.0	0.0	-0.29568	0.0	1.1048	0.0

V. CLASSICAL ROTATIONAL TRAJECTORIES

Given the moments of inertia computed from the equilibrium coordinates of the water molecule as shown in Section III above, we could straightforwardly compute the rotational spectrum[3,5,6] quantum mechanically in the rigid rotor approximation. Instead, in order to gain more intuitive insight into the physical basis of infrared and Raman band contours, and to make more evident the connection to the liquid state, we compute the band contours from classical mechanics, using a method improved over the asymmetric rotor techniques pioneered by Bratos, Guissani, and Leicknam.[49-56] The methodology presented in Sections V-VII allows the rapid and accurate calculation of classical rigid rotor infrared and Raman band contours for any molecule, including asymmetric rotors like water. (For examples of earlier less general treatments for linear, spherical, and symmetric tops, see St. Pierre and Steele[57] and references therein as well as references in the asymmetric rotor papers of Bratos, Guissani, and Leicknam.[49-56]) The method presented here is simple and direct, involving no reference to Euler angles or special functions. Approximate sets of infrared and Raman contours can be computed in one minute on a VAX[58] 11/780 and very accurate sets in 15 minutes. The rotational functions discussed here require only a 250 line program plus standard integration and fast Fourier transform routines. In the rest of this section we develop the techniques to efficiently compute the necessary rotational properties.

In order to calculate rotational trajectories we choose a set of body fixed axes coinciding with the principle axes of the molecule, those axes of a rigid body for which the moment of inertia tensor is diagonal. The center of mass is at the origin of both the space fixed and body fixed coordinate systems; thus, the relationship between the two sets of axes is specified by their relative orientation. This orientation is usually expressed in terms of the Euler angles ϕ,θ, and ψ, but for our purposes (particularly the numerical aspects) it is more convenient to use the Cartesian rotation matrix $\mathbf{D}$ in terms of direction cosines (for an alternative treatment using Euler angles and special functions, see the work of Bratos, Guissani, and Leickman[49-56]). If $\mathbf{a}$ is a vector in terms of the space fixed axes, and $\mathbf{a}'$ is the vector in terms of the body fixed axes, then $\mathbf{a}$ is related to $\mathbf{a}'$ by $\mathbf{a} = \mathbf{D}\mathbf{a}'$. Similarly, if $\mathbf{T}$ is a tensor, we have $\mathbf{T} = \mathbf{D}\mathbf{T}'\mathbf{D}^{-1}$. The time history of the orientation of the molecule is given by $\mathbf{D}(t)$.

We now derive equations of motion for $\mathbf{D}(t)$. While the results are not new, the following derivation is simple and serves to introduce the notation used in later parts of the paper. Let $\hat{\mathbf{e}}_i$, $i=1,2,3$, be the unit vectors in the x, y, and z space fixed directions, and similarly let $\hat{\mathbf{E}}_\alpha(t)$, $\alpha=1,2,3$, be the time varying body fixed unit vectors. Note that we use lower case Roman letters for indices taking on values associated with the space frame, and lower case Greek letters for body frame indices. The components of $\mathbf{D}(t)$, $D_{i\alpha}(t)$, are given by

$$D_{i\alpha}(t) = \hat{\mathbf{e}}_i \cdot \hat{\mathbf{E}}_\alpha(t) \,. \tag{5.1}$$

Let $\boldsymbol{\omega}(t)$ be the angular velocity vector and $\omega_\alpha(t)$ be its components in the body frame, so that, adopting here and in the rest of the paper (except where otherwise noted), the convention that repeated indices on different symbols are to be summed over, $\boldsymbol{\omega}(t) = \omega_\alpha(t)\hat{\mathbf{E}}_\alpha(t)$. If we let $\mathbf{L}$ be the angular momentum, and $\mathbf{I}$ be the moment of inertia tensor, then $\mathbf{L} = \mathbf{I}\boldsymbol{\omega}$, or

$$\mathbf{L} = I_{\alpha\beta}\,\omega_\beta(t)\hat{\mathbf{E}}_\alpha(t), \tag{5.2}$$

where $I_{\alpha\beta}$ are the components of $\mathbf{I}$ in the body axes, and thus do not vary in time in our rigid body approximation. Since for our isolated system there are no external torques,

$$\frac{d\mathbf{L}}{dt} = I_{\alpha\beta}\left[\frac{d\omega_\beta(t)}{dt}\hat{\mathbf{E}}_\alpha(t) + \omega_\beta(t)\frac{d\hat{\mathbf{E}}_\alpha(t)}{dt}\right] = 0. \tag{5.3}$$

Since the $\hat{\mathbf{E}}_\alpha$ are fixed in the body frame,

$$\frac{d\hat{\mathbf{E}}_\alpha}{dt} = \boldsymbol{\omega}\times\hat{\mathbf{E}}_\alpha = \omega_\mu \epsilon_{\mu\alpha\gamma}\hat{\mathbf{E}}_\gamma \,. \tag{5.4}$$

Here $\epsilon_{\mu\alpha\gamma}$ is the permutation symbol or Levi-Civita density,[59] defined to be zero if any two of its indices are equal, and otherwise +1 or −1 according to whether $\mu\alpha\gamma$ is an even or odd permutation respectively of 1,2,3. Using this relationship and Eq. (5.3) we obtain

$$I_{\alpha\beta}\frac{d\omega_\beta}{dt} + I_{\gamma\beta}\,\omega_\beta\,\omega_\mu\,\epsilon_{\mu\gamma\alpha} = 0. \tag{5.5}$$

For our chosen set of body axes the inertia tensor is diagonal, so this reduces to Euler's equations of motion for a rigid body free of external torques:

$$I_{xx}\frac{d\omega_x}{dt} + \omega_y\omega_z(I_{zz} - I_{yy}) = 0,$$

$$I_{yy}\frac{d\omega_y}{dt} + \omega_z\omega_x(I_{xx} - I_{zz}) = 0, \tag{5.6}$$

$$I_{zz}\frac{d\omega_z}{dt} + \omega_x\omega_y(I_{yy} - I_{xx}) = 0.$$

We similarly obtain from Eqs. (5.1) and (5.4)

$$\frac{d}{dt}D_{i\alpha} = \hat{\mathbf{e}}_i\cdot\frac{d}{dt}\hat{\mathbf{E}}_\alpha = \omega_\beta\epsilon_{\alpha\gamma\beta}D_{i\gamma} \tag{5.7}$$

as the equations of motion for $D_{i\alpha}$.

In order to calculate infrared and Raman rotational and vibrational-rotational spectral band contours with this classical rigid rotor method, we will show in Sections VI and VII below that we must separate an ensemble average of an autocorrelation function of the dipole moment $\boldsymbol{\mu}$ for the infrared case and the polarizability tensor $\mathbf{P}$ for the Raman case into a product of ensemble averages. One of these ensemble averages is an average over vibrational states of an autocorrelation function of $\boldsymbol{\mu}$ or $\mathbf{P}$, and the other is a rotational ensemble average of elements of a rotation matrix over initial angular velocity and initial orientation. With Eqs. (5.6) and (5.7) we have at all that we need, in principle, to calculate numerically the rotational ensemble averages necessary to compute the rigid body rotational part of the spectra, but we can save ourselves a large amount of computer time and increase our understanding of the dependence of band shape on the moment of inertia tensor and temperature by doing part of the problem analytically.

With Eqs. (5.6) and (5.7), $\mathbf{D}(t)$ is determined by the initial values of $\mathbf{D}$ and $\boldsymbol{\omega}$, i.e. $\mathbf{D}^0$ and $\boldsymbol{\omega}^0$, while $\boldsymbol{\omega}(t)$ is determined solely by $\boldsymbol{\omega}^0$. Thus we write $\mathbf{D}(t,\mathbf{D}^0,\boldsymbol{\omega}^0)$ and $\boldsymbol{\omega}(t,\boldsymbol{\omega}^0)$. If the pair $\mathbf{D}(t,\mathbf{D}^0,\boldsymbol{\omega}^0)$ and $\boldsymbol{\omega}(t,\boldsymbol{\omega}^0)$ together satisfy the equations of motion, then by the isotropy of space, so do $\mathbf{R}\mathbf{D}(t,\mathbf{D}^0,\boldsymbol{\omega}^0)$ and $\boldsymbol{\omega}(t,\boldsymbol{\omega}^0)$, where $\mathbf{R}$ is any rotation. Accordingly we introduce a rotational Green's function $\mathbf{G}(t)$ with the following definition:

$$\mathbf{G}(t,\boldsymbol{\omega}^0) \equiv \mathbf{D}(t,\mathbf{1},\boldsymbol{\omega}^0)\ . \tag{5.8}$$

in which $\mathbf{1}$ is the unit matrix. It follows that since $\mathbf{D}(t,\mathbf{D}^0,\boldsymbol{\omega}^0)$ and $\mathbf{D}^0\mathbf{G}(t,\boldsymbol{\omega}^0)$ satisfy the same equations of motion, and have the same initial conditions, then

$$\mathbf{D}(t,\mathbf{D}^0,\boldsymbol{\omega}^0) = \mathbf{D}^0\mathbf{G}(t,\boldsymbol{\omega}^0)\ . \tag{5.9}$$

$\mathbf{G}(t)$ may be viewed as a rotational propagator acting on the initial orientation $\mathbf{D}^0$. $\mathbf{G}(t)$ is the rotation matrix as a function of time assuming that the initial body fixed axes coincide with the space fixed axes. $\mathbf{D}^0$ then rotates this trajectory to make it coincide with the actual initial orientation. This separation will allow us to analytically perform ensemble averages over initial orientations, as we will show in Sections VI and VII below. The rotational ensemble average for $\mathbf{G}$ then reduces to an ensemble average over $\boldsymbol{\omega}^0$.

As we will show below in Section VI, in order to calculate infrared spectra we need to calculate the time history of $<G_{\alpha\beta}(t)>$. Here $< >$ indicates an ensemble average over a Boltzmann distribution of initial angular velocities. For Raman spectra, as we will show in Section VII, we need to calculate the time history of $<G_{\alpha\beta}(t)G_{\gamma\delta}(t)>$. Using Eqs. (5.6) and (5.7) we could calculate these elements as they stand. A naive approach would be to choose a grid in $\boldsymbol{\omega}$ space of initial $\boldsymbol{\omega}$'s, calculate the various elements and products of $\mathbf{G}(t)$ for a set of t's, weight them by the appropriate Boltzmann factor and then sum. (Note that the equations of motion for $\mathbf{G}$ and $\mathbf{D}$ are the same, since they differ only by initial conditions.) Although the averaging over initial orientations is done analytically, the computer time required for this calculation would be large, but fortunately a variety of simplifications are possible.

Our ensemble average over initial angular velocity is given by

$$<G(t)> = \int_{-\infty}^{\infty}\int_{-\infty}^{\infty}\int_{-\infty}^{\infty} P(\omega_x^0,\omega_y^0,\omega_z^0)G(t,\boldsymbol{\omega}^0)d\omega_x^0 d\omega_y^0 d\omega_z^0\ , \tag{5.10}$$

where $G(t)$ stands for a term of the form $G_{\alpha\beta}(t)$ for infrared spectra or $G_{\alpha\beta}(t)G_{\gamma\delta}(t)$ for Raman spectra, and $P(\omega_x^0,\omega_y^0,\omega_z^0)$ is the Boltzmann probability density, which as we show in Appendix A, is given by

$$P(\omega_x^0,\omega_y^0,\omega_z^0) = C\exp\left[-\tfrac{1}{2}\beta[I_{xx}(\omega_x^0)^2 + I_{yy}(\omega_y^0)^2 + I_{zz}(\omega_z^0)^2]\right] , \tag{5.11}$$

where C is a normalizing constant, $\beta=(k_B T)^{-1}$, k_B is Boltzmann's constant, and T is the temperature. We can simplify this probability density by changing variables to $u_\alpha = \sqrt{I_{\alpha\alpha}}\omega_\alpha$ (no summation). We then have

$$P(u_x,u_y,u_z) = C'\exp\left[-\tfrac{1}{2}\beta(u_x^2 + u_y^2 + u_z^2)\right] , \tag{5.12}$$

in which C' is a new constant. This probability distribution is now spherically symmetric, so we let $u^2 = u_x^2 + u_y^2 + u_z^2$, and change variables again to get

$$P(u,\Omega) = C''\, u^2\exp\left[-\tfrac{1}{2}\beta u^2\right] , \tag{5.13}$$

where Ω is the solid angle, i.e. orientation, of the vector (u_x,u_y,u_z). The ensemble average then becomes

$$<G(t)> = C''\int_0^\infty u^2 e^{-\frac{1}{2}\beta u^2}\int G(t,u,\Omega)\,d\Omega\ du , \tag{5.14}$$

where $G(t,u,\Omega)$ is $G(t)$ with the initial value $\boldsymbol{\omega}^0$ specified by u and Ω. This change of variables in the probability density means that we separate the integration over the magnitude of $\boldsymbol{\omega}^0$ from the integration over the direction of $\boldsymbol{\omega}^0$. This in turn will allow us to use the scaling properties of $\boldsymbol{\omega}$ and G to change the integral over the magnitude of $\boldsymbol{\omega}$ to an integral over time, which will mean that the work in calculating the time history of $G(t)$ and doing the integral will overlap.

We do this as follows: we first note that solutions to our equations of motion are unique for given initial conditions. If we have two solutions which have the same initial conditions, then they must be equal. Using this property, we will derive scaling relations between t and $\boldsymbol{\omega}^0$, first for $\boldsymbol{\omega}$, and then for G.

Suppose $\boldsymbol{\omega}(t,\boldsymbol{\omega}^0)$ satisfies Eqs. (5.6). Then it is not difficult to check that $\alpha\boldsymbol{\omega}(\alpha t,\boldsymbol{\omega}^0)$ also satisfies Eqs. (5.6), where α is an arbitrary scalar constant. The initial conditions for $\boldsymbol{\omega}$ tell us that $\alpha\boldsymbol{\omega}(0,\boldsymbol{\omega}^0) = \alpha\boldsymbol{\omega}^0$. By definition, $\boldsymbol{\omega}(t,\alpha\boldsymbol{\omega}^0)$ is the solution to Eqs. (5.6) for the initial value $\alpha\boldsymbol{\omega}^0$. We conclude that

$$\boldsymbol{\omega}(t,\alpha\boldsymbol{\omega}^0) = \alpha\boldsymbol{\omega}(\alpha t,\boldsymbol{\omega}^0) . \tag{5.15}$$

The intuitive picture for this is as follows: suppose we allow two identical rigid bodies to rotate subject to the same initial conditions, except that one starts with an initial angular velocity in the same direction as the other but with a magnitude larger by a factor α. This equation tells us that the two bodies will follow the same rotational trajectory through $\boldsymbol{\omega}$-space, except that one will trace its path more quickly by the factor α and its magnitude will be greater by the factor α. Using this relation we can in a very similar manner show that

$$\mathrm{G}(\alpha t,\boldsymbol{\omega}^0) = \mathrm{G}(t,\alpha\boldsymbol{\omega}^0) . \tag{5.16}$$

This relationship tells us that our two identical bodies with different initial $\boldsymbol{\omega}$'s will trace the same path through orientation space (without scaling the magnitude of G), except that one will trace its path more quickly by the factor α. We now change variables in Eq. (5.14) from u to ξ, with $u = u^0\xi$, where ξ is a unitless integration variable, and where we choose u_0 to be the value of u at the maximum of $P(u,\Omega)$, so that $u_0 = (2/\beta)^{\frac{1}{2}}$. We obtain

$$<G(t)> = C''\int_0^\infty u_0^3\xi^2 e^{-\frac{1}{2}\beta u_0^2\xi^2}\int G(t,u_0\xi,\Omega)\,d\Omega\, d\xi , \tag{5.17}$$

where the left integral is over ξ from 0 to ∞ and the right integral carries Ω over the sphere. Eq. (5.16) tells us that

$$G(t,u_0\xi,\Omega) = G(\xi t,u_0,\Omega) , \tag{5.18}$$

so we have

$$<G(t)> = (\frac{\beta}{2\pi})^{\frac{3}{2}}\int_0^\infty u_0^3 \xi^2 e^{-\frac{1}{2}\beta u_0^2 \xi^2}\int G(\xi t,u_0,\Omega)d\Omega d\xi , \tag{5.19}$$

where we now explicitly write out the normalizing constant C^*. Written in this way, the work necessary to compute the time history and to compute the time integral overlap almost completely.

By various symmetry arguments relating to the molecule's inertia tensor (which are valid because in the body frame the inertia tensor is diagonal) we show in Appendix B that the off-diagonal elements of $<G_{\alpha\beta}(t)>$ are zero. We also show that the only non-zero elements of $<G_{\alpha\beta}(t)G_{\gamma\delta}(t)>$ are those having indices which come in pairs, i.e., if any index is unique and not matched by some other index, then $<G_{\alpha\beta}(t)G_{\gamma\delta}(t)> = 0$. Another result of these symmetry considerations is that one need only do the integration over the sphere for two adjacent octants, saving a factor of four in computation time.

We carry out our computation as follows: first we perform the integration over Ω. Using a product Gaussian quadrature method for numerical integration on the sphere,[60] we choose a set of initial directions Ω for the scaled initial angular velocity, restricting the integration to two adjacent octants. For each direction Ω we compute the time histories of the elements $G_{\alpha\beta}(\xi t,u_0,\Omega)$ using Eqs. (5.6) and (5.7) and a variable order, variable time step numerical integrator[61] for the single selected u_0, adding together the different time histories corresponding to different Ωs with their proper weights,[60] averaging them together as we proceed to form a single set of time histories $G_{\alpha\alpha}(\xi t,u_0)$ for the infrared case and $G_{\alpha\beta}(\xi t,u_0)G_{\gamma\delta}(\xi t,u_0)$ for the Raman case, i.e., we evaluate

$$G_{\alpha\alpha}(\xi t,u_0) = \int G_{\alpha\alpha}(\xi t,u_0,\Omega)d\Omega \tag{5.20}$$

and

$$G_{\alpha\beta}(\xi t,u_0)G_{\gamma\delta}(\xi t,u_0) = \int G_{\alpha\beta}(\xi t,u_0,\Omega)G_{\gamma\delta}(\xi t,u_0,\Omega)d\Omega . \tag{5.21}$$

To compute the final $<G_{\alpha\alpha}(t)>$ and $<G_{\alpha\beta}(t)G_{\gamma\delta}(t)>$ we now integrate the stored $<G_{\alpha\alpha}(\xi t,u_0)>$ and $<G_{\alpha\beta}(\xi t,u_0)G_{\gamma\delta}(\xi t,u_0)>$ over ξ as shown in Eq. (5.19).

These free rotor results may also be extended[49-56] to treat various rotational diffusion models.

In Fig. 3 we present $<G_{\alpha\alpha}(t)>$ for $\alpha = x,y,z$, along with their Fourier transforms, for H_2O. All relevant parameters for the molecule are calculated *ab initio*, the moment of inertia tensor being derived from the *ab initio* equilibrium geometry. The fact that G_{yy} does not tend to zero for large t indicates that a water molecule can rotate for long periods about its smallest moment of inertia, which is then reflected in the delta function Q branch seen in its Fourier transform, also shown in Fig. 3.

VI. INFRARED SPECTRA

We now derive the appropriate equations for *ab initio* computation of infrared spectral band contours. While nothing in this section is basically new (for example see the work of Gordon,[16, 18] of Bratos, Guissani, and Leicknam,[49-56] and our earlier papers,[1, 2]), we derive here in one place the various equations needed for the different approaches discussed in this paper. We first obtain equations appropriate for a *simultaneous* full quantum force classical trajectory (QFCT) spectral computation, and then derive equations for the separation of vibration and rotation and the treatment of rotation in a fully classical rigid rotor approximation, for both *simultaneous* and *sequential* approaches. Finally we show the equations for the *sequential* rigid

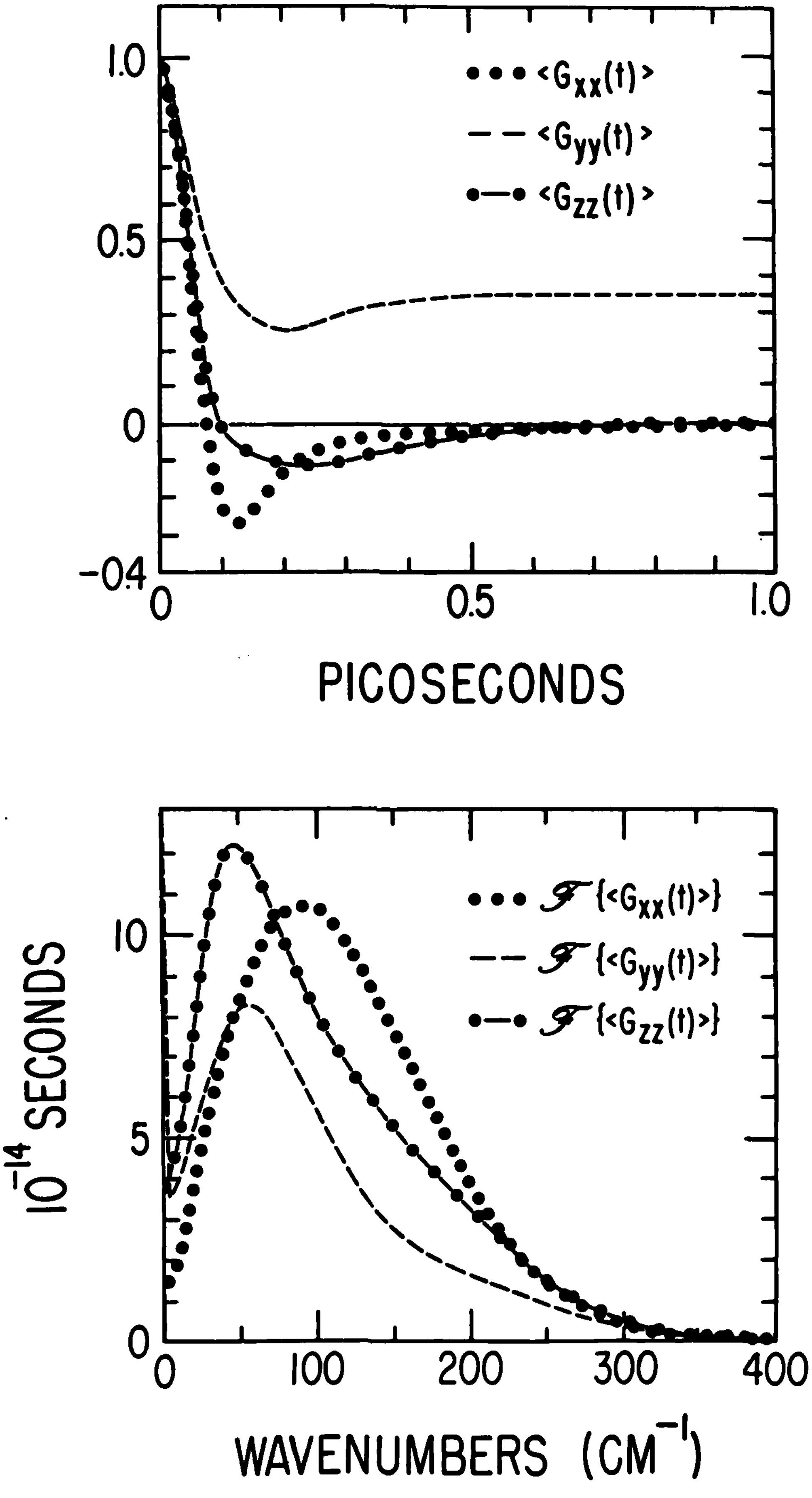

Figure 3. In the upper panel we show for H_2O the time histories of the ensemble averaged rigid rotor vectorial correlation function $<G_{\alpha\alpha}(t)>$ for $\alpha = x,y,z$. In the lower panel we show the corresponding Fourier transforms $F\{<G_{\alpha\alpha}(t)>\}$ which produce the infrared pure rotational and vibrational rotational bandshapes. The delta function in the Fourier transform at zero frequency (wavenumbers) appears only for $\alpha = y$, the axis with the smallest moment of inertia, and arises from the finite long time limit of $<G_{yy}(t)>$, shown in the upper panel.

rotor, normal mode approximation.

We start with the following linear response theory equations from Gordon[1,16,18] giving the equilibrium infrared spectrum as

$$\alpha(\omega) = \frac{4\pi^2\omega[1 - e^{-\beta\hbar\omega}]}{3\hbar cn} I(\omega) , \tag{6.1}$$

$$I(\omega) = (2\pi)^{-1}\int_{-\infty}^{\infty} dt\, e^{-i\omega t} \langle \tilde{\mu}(0)\cdot\tilde{\mu}(t)\rangle , \tag{6.2}$$

in which $\alpha(\omega)$ is the absorption cross section as a function of frequency ω (not to be confused with the angular velocity vector $\boldsymbol{\omega}$), $\beta=(k_B T)^{-1}$ in which k_B is Boltzmann's constant and T the temperature, $\hbar=h/2\pi$ in which h is Planck's constant, c is the speed of light, n is the index of refraction of the medium, $I(\omega)$ is defined as the absorption lineshape and is evaluated for an isotropic medium, and $\langle\tilde{\mu}(0)\cdot\tilde{\mu}(t)\rangle$ is the ensemble average of the space fixed dipole moment time autocorrelation function. We now use tildes over the dipole moment vectors $\tilde{\mu}$ to differentiate these space fixed dipole moments from the body fixed dipole moments to follow, which we will write without the tilde, as μ. Denoting the Fourier transform by F, we can write $I(\omega)$ as

$$I(\omega) = (2\pi)^{-1}F\{\langle\tilde{\mu}(0)\cdot\tilde{\mu}(t)\rangle\} , \tag{6.3}$$

where we define the Fourier transform as

$$F f(t) = \int_{-\infty}^{\infty} e^{-i\omega t} f(t)\, dt . \tag{6.4}$$

We can also express Eq. (6.2) in terms of the power spectrum[1]

$$I(\omega) = (2\pi)^{-1}\left\langle \lim_{\tau\to\infty}\frac{1}{2\tau}\sum_{j=x,y,z}\left|\int_{-\tau}^{\tau} dt\, e^{-i\omega t}\tilde{\mu}_j(t)\right|^2\right\rangle . \tag{6.5}$$

where an average is assumed over a proper ensemble of trajectories. Given an ensemble of time histories of $\tilde{\mu}(t)$from *simultaneous* QFCT calculations, we can use Eqs. (6.1) and (6.2) or (6.5) to compute the infrared spectrum.[1]

We now take the rigid rotor, vibrator approximation that the dipole moment can be written as $\tilde{\mu}(t) = \mathbf{D}(t)\mu(t)$, where $\tilde{\mu}(t)$ is the space fixed dipole moment, $\mathbf{D}(t)$ is the rotation matrix transforming a vector relative to the body fixed frame to a vector relative to space fixed axes, and $\mu(t)$ is the dipole moment in the body frame. Expressing this in terms of components, we have (again using the summation convention that repeated indices on different symbols are to be summed over)

$$\tilde{\mu}_i(t) = D_{i\alpha}(t)\mu_\alpha(t) , \tag{6.6}$$

$$I(\omega) = (2\pi)^{-1}F\{\langle D_{i\alpha}(0)\mu_\alpha(0)D_{i\beta}(t)\mu_\beta(t)\rangle\} . \tag{6.7}$$

We note that because of the linearity of both the Fourier transform and the ensemble average, we are free to take the implied summations in Eq. (6.7) wherever we wish.

We take the rigid rotor, vibrator approximation that vibration and rotation are uncoupled and uncorrelated, and thus we may take their ensemble averages separately

$$I(\omega) = (2\pi)^{-1}F\{\langle D_{i\alpha}(0)D_{i\beta}(t)\rangle\langle\mu_\alpha(0)\mu_\beta(t)\rangle\} . \tag{6.8}$$

In order to take advantage of the rotational isotropy of space as discussed in Section V above, we write $\mathbf{D}(t)$ as

$$\mathbf{D}(t) = \mathbf{D}(0)\mathbf{G}(t) . \tag{6.9}$$

We now have

$$I(\omega) = (2\pi)^{-1}\, F\{\langle D_{i\alpha}(0)D_{i\gamma}(0)G_{\gamma\beta}(t)\rangle\langle\mu_\alpha(0)\mu_\beta(t)\rangle\} . \tag{6.10}$$

Because D is orthogonal, $D_{i\alpha}D_{i\gamma} = \delta_{\alpha\gamma}$, and we have

$$I(\omega) = (2\pi)^{-1} F\{<G_{\alpha\beta}(t)><\mu_\alpha(0)\mu_\beta(t)>\} \,. \tag{6.11}$$

As we show in Appendix B, the off-diagonal components of $<G_{\alpha\beta}(t)>$ are zero. Accordingly, we have (making the summation explicit now)

$$I(\omega) = (2\pi)^{-1} \sum_{\alpha=x,y,z} F\{<G_{\alpha\alpha}(t)><\mu_\alpha(0)\mu_\alpha(t)>\} \,. \tag{6.12}$$

This can also be written in the following two ways:[62]

$$I(\omega) = (2\pi)^{-1} \sum_{\alpha=x,y,z} F\{<G_{\alpha\alpha}(t)>\} * F\{<\mu_\alpha(0)\mu_\alpha(t)>\} \tag{6.13}$$

and

$$I(\omega) = (2\pi)^{-1} \sum_{\alpha=x,y,z} F\{<G_{\alpha\alpha}(t)>\} * <\lim_{\tau\to\infty} \frac{1}{2\tau} \left| \int_{-\tau}^{\tau} dt e^{-i\omega t} \mu_\alpha(t) \right|^2 > \,, \tag{6.14}$$

where * denotes convolution defined as

$$f * g \ (\omega) = (2\pi)^{-1} \int_{-\infty}^{\infty} f(\omega - \omega')g(\omega')d\omega' \,. \tag{6.15}$$

Eqs. (6.1) and (6.13) or (6.14) are appropriate for a *simultaneous* QFCT rigid rotor, vibrator approach in which we compute the classical vibrational trajectories $\mu_\alpha(t)$ in body fixed coordinates and then convolve with the rigid rotor rotational band shapes $F\{<G_{\alpha\alpha}(t)>\}$. In order to carry out a *sequential* rigid rotor, normal mode analysis, in Appendix C we evaluate the vibrational correlation function $F\{<\mu_\alpha(0)\mu_\alpha(t)>\}$ in terms of normal coordinate derivatives. Using those results, we obtain

$$I(\omega) = \sum_{\alpha=x,y,z} F\{<G_{\alpha\alpha}(t)>\} * \left[(\mu_\alpha^0)^2\delta(\omega) + \sum_{j=1}^{3} (\frac{\partial\mu_\alpha}{\partial q_j})^2 \frac{\hbar}{2\omega_j} \frac{\delta(\omega_j - \omega)}{1 - \exp(-\beta\hbar\omega)} \right] , \tag{6.16}$$

where μ_α^0 is the equilibrium value of μ_α, $\delta(\omega)$ is the Dirac delta function, q_j is a normal coordinate, and ω_j is the frequency of the jth normal mode. The factor to the left of the * in the convolution is responsible for the bandshapes, while the factor in brackets to the right specifies the frequencies and intensities of the pure rotational and vibrational bands.

It is necessary to apply a detailed balance quantum correction[1] to the classical rotational results for all the approaches given above. The infrared rotational and vibrational-rotational bands for equilibrium systems thus are corrected by multiplying the intensities by

$$\exp[\beta\hbar(\Delta\omega)/2] \,, \tag{6.17}$$

in which $\beta = (k_B T)^{-1}$, k_B is Boltzmann's constant and $\Delta\omega$ is the displacement from the rotationless band center ($\Delta\omega = \omega$ for pure rotational). No quantum corrections are necessary for the vibrational intensities when they are calculated quantum mechanically as in Eq. (6.16). If the vibrational motion is treated as a classical trajectory, as in Eqs. (6.3), (6.5) or (6.14), then the vibrational rotational band intensities can be multiplied by the harmonic quantum correction factor[1]

$$\frac{\beta\hbar\omega}{1 - \exp(-\beta\hbar\omega)} \,, \tag{6.18}$$

part of which cancels out a similar factor in Eq. (6.1).

VII. RAMAN SPECTRA

We proceed in the Raman case as we did for the infrared. First we derive equations appropriate for a *simultaneous* QFCT calculation, then from this we obtain equations appropriate for a separation of rotational from vibrational motion and finally we derive the equations for the more usual rigid rotor, normal mode *sequential* calculation following the lines described by Bratos, Guissani, and Leicknam.[49-56] We begin with the linear response equations for Raman spectra[2,14,16,18]

$$\left(\bar{\lambda}_i \bar{\lambda}_s^3 \frac{d^2\sigma}{d\omega d\Omega}\right)_{iso} = (2\pi)^{-1}\int_{-\infty}^{\infty} dt\ \exp(-i\omega t)\tfrac{1}{3}<\mathrm{Tr}\left[\tilde{\mathbf{P}}^{iso}(0)\tilde{\mathbf{P}}^{iso}(t)\right]> \tag{7.1}$$

$$\left(\bar{\lambda}_i \bar{\lambda}_s^3 \frac{d^2\sigma}{d\omega d\Omega}\right)_{an} = (2\pi)^{-1}\int_{-\infty}^{\infty} dt\ \exp(-i\omega t)<\mathrm{Tr}\left[\tilde{\mathbf{P}}^{an}(0)\tilde{\mathbf{P}}^{an}(t)\right]>, \tag{7.2}$$

in which Eqs. (7.1) and (7.2) are the differential cross sections for scattering into angular frequency range $d\omega$ and solid angle range $d\Omega$ for the isotropic and anisotropic Raman spectra, respectively, weighted by $\bar{\lambda}_i$, in which $2\pi\bar{\lambda}_i$ is the wavelength of the incident radiation, and by $\bar{\lambda}_s^3$, in which $2\pi\bar{\lambda}_s$ is the wavelength of the scattered radiation.[63] $\tilde{\mathbf{P}}$ is the space fixed Cartesian polarizability tensor, $\tilde{\mathbf{P}}^{iso} = \tilde{P}^{iso}\mathbf{1}$ is its isotropic part, where $\tilde{P}^{iso} = \frac{1}{3}(\mathrm{Tr}\tilde{\mathbf{P}})$ and $\mathbf{1}$ is the identity tensor, $\tilde{\mathbf{P}}^{an} = \tilde{\mathbf{P}} - \tilde{\mathbf{P}}^{iso}$ is its anisotropic part, Tr indicates trace, and it is understood that the correlation functions in Eqs. (7.1) and (7.2) are averaged over the desired ensemble. We now use tildes over the polarizability tensors $\tilde{\mathbf{P}}$ to differentiate these space fixed polarizabilities from the body fixed polarizabilities to follow, which we will write without the tilde, as $\mathbf{P}$. We can also express Eqs. (7.1) and (7.2) in terms of the power spectrum[2]

$$\left(\bar{\lambda}_i \bar{\lambda}_s^3 \frac{d^2\sigma}{d\omega d\Omega}\right)_{iso} = (2\pi)^{-1}<\lim_{\tau\to\infty}\frac{1}{2\tau}\left|\int_{-\tau}^{\tau} dt\ e^{-i\omega t}\ \tilde{P}^{iso}(t)\right|^2>. \tag{7.3}$$

$$\left(\bar{\lambda}_i \bar{\lambda}_s^3 \frac{d^2\sigma}{d\omega d\Omega}\right)_{an} = (2\pi)^{-1}\sum_{i,j}<\lim_{\tau\to\infty}\frac{1}{2\tau}\left|\int_{-\tau}^{\tau} dt\ e^{-i\omega t}\tilde{P}_{ij}^{an}(t)\right|^2>, \tag{7.4}$$

where averaging over the proper ensemble of trajectories is assumed. Given an ensemble of $\tilde{\mathbf{P}}(t)$ time histories from *simultaneous* QFCT calculations, we can use Eqs. (7.1) and (7.2) or (7.3) and (7.4) to compute the Raman spectrum.

For both the isotropic and anisotropic cases we wish to evaluate time correlation functions of the form $<\mathrm{Tr}[\tilde{\mathbf{P}}(0)\tilde{\mathbf{P}}(t)]>$. Employing the summation convention once again, we write

$$<\mathrm{Tr}[\tilde{\mathbf{P}}(0)\tilde{\mathbf{P}}(t)]> = <\tilde{P}_{ik}(0)\tilde{P}_{ki}(t)>. \tag{7.5}$$

As in the infrared case, we take the rigid rotor, vibrator approximation and write

$$\tilde{P}_{ik}(t) = D_{i\alpha}(t)P_{\alpha\beta}(t)D_{\beta k}^{-1}(t), \tag{7.6}$$

where $\tilde{\mathbf{P}}$ is the space fixed and $\mathbf{P}$ is the body fixed polarizability tensor. Then

$$<\mathrm{Tr}[\tilde{\mathbf{P}}(0)\tilde{\mathbf{P}}(t)]> = <D_{i\alpha}(0)P_{\alpha\beta}(0)D_{\beta k}^{-1}(0)D_{k\gamma}(t)P_{\gamma\delta}(t)D_{\delta i}^{-1}(t)>. \tag{7.7}$$

Separating vibration and rotation as before, we have

$$<\mathrm{Tr}[\tilde{\mathbf{P}}(0)\tilde{\mathbf{P}}(t)]> = <D_{i\alpha}(0)D_{\beta k}^{-1}(0)D_{k\gamma}(t)D_{\delta i}^{-1}(t)><P_{\alpha\beta}(0)P_{\gamma\delta}(t)>. \tag{7.8}$$

As in the infrared case, we may write $\mathbf{D}(t) = \mathbf{D}(0)\mathbf{G}(t)$, where $\mathbf{G}(t)$ is the rotational Green's Function. Making use of the fact that, because rotation matrices are orthogonal, $D_{\delta j}^{-1}(t) = D_{j\delta}(t)$, we write

$$\begin{aligned}<\mathrm{Tr}[\tilde{\mathbf{P}}(0)\tilde{\mathbf{P}}(t)]> &= <D_{i\alpha}(0)D_{\beta k}^{-1}(0)D_{k\mu}(0)G_{\mu\gamma}(t)D_{i\nu}(0)G_{\nu\delta}(t)><P_{\alpha\beta}(0)P_{\gamma\delta}(t)> \\ &= <D_{i\alpha}(0)D_{\beta k}^{-1}(0)D_{k\mu}(0)D_{i\nu}(0)><G_{\mu\gamma}(t)G_{\nu\delta}(t)><P_{\alpha\beta}(0)P_{\gamma\delta}(t)>.\end{aligned} \tag{7.9}$$

Since $\mathbf{D}^{-1}(0)\mathbf{D}(0) = \mathbf{1}$, the unit matrix, $D_{\beta k}^{-1}(0)D_{k\mu}(0) = \delta_{\beta\mu}$, and because $\mathbf{D}$ is orthogonal, $D_{i\alpha}(0)D_{i\nu}(0) = \delta_{\alpha\nu}$, and thus we have

$$<\mathrm{Tr}[\tilde{\mathbf{P}}(0)\tilde{\mathbf{P}}(t)]> = \ <G_{\beta\gamma}(t)G_{\alpha\delta}(t)><P_{\alpha\beta}(0)P_{\gamma\delta}(t)> \ . \tag{7.10}$$

We now make use of the relation $P_{\alpha\beta} = P^{iso}\delta_{\alpha\beta} + P^{an}_{\alpha\beta}$ to write Eqs. (7.1) and (7.2) as

$$\left(\bar{\lambda}_i\bar{\lambda}_s^3 \frac{d^2\sigma}{d\omega d\Omega}\right)_{iso} = (6\pi)^{-1}F\{\ <G_{\beta\gamma}(t)G_{\alpha\delta}(t)><P^{iso}(0)\delta_{\alpha\beta}P^{iso}(t)\delta_{\gamma\delta}>\ \} \tag{7.11}$$

$$\left(\bar{\lambda}_i\bar{\lambda}_s^3 \frac{d^2\sigma}{d\omega d\Omega}\right)_{an} = (2\pi)^{-1}F\{\ <G_{\beta\gamma}(t)G_{\alpha\delta}(t)><P^{an}_{\alpha\beta}(0)P^{an}_{\gamma\delta}(t)>\ \}\ . \tag{7.12}$$

We can also write these as

$$\left(\bar{\lambda}_i\bar{\lambda}_s^3 \frac{d^2\sigma}{d\omega d\Omega}\right)_{iso} = (6\pi)^{-1}F\{\ <G_{\beta\gamma}(t)G_{\alpha\delta}(t)>\} * F\{<P^{iso}(0)\delta_{\alpha\beta}P^{iso}(t)\delta_{\gamma\delta}>\ \}\ . \tag{7.13}$$

$$\left(\bar{\lambda}_i\bar{\lambda}_s^3 \frac{d^2\sigma}{d\omega d\Omega}\right)_{an} = (2\pi)^{-1}F\{\ <G_{\beta\gamma}(t)G_{\alpha\delta}(t)>\} * F\{<P^{an}_{\alpha\beta}(0)P^{an}_{\gamma\delta}(t)>\ \}\ . \tag{7.14}$$

and[62]

$$\left(\bar{\lambda}_i\bar{\lambda}_s^3 \frac{d^2\sigma}{d\omega d\Omega}\right)_{iso} = (6\pi)^{-1}F\{\ <G_{\beta\gamma}(t)G_{\alpha\delta}(t)>\} *$$

$$<\lim_{\tau\to\infty}\frac{1}{2\tau}\left|\int_{-\tau}^{\tau} dt e^{-i\omega t}P^{iso}(t)\right|^2 \delta_{\alpha\beta}\delta_{\gamma\delta}>\ . \tag{7.15}$$

$$\left(\bar{\lambda}_i\bar{\lambda}_s^3 \frac{d^2\sigma}{d\omega d\Omega}\right)_{an} = (2\pi)^{-1}F\{\ <G_{\beta\gamma}(t)G_{\alpha\delta}(t)>\} *$$

$$<\lim_{\tau\to\infty}\frac{1}{2\tau}\left(\int_{-\tau}^{\tau} dt e^{-i\omega t}P^{an}_{\alpha\beta}(t)\right)^{\dagger}\left(\int_{-\tau}^{\tau} dt e^{-i\omega t}P^{an}_{\gamma\delta}(t)\right)>\ . \tag{7.16}$$

where the $\dagger$ is used here to indicate complex conjugation.

Eqs. (7.13) and (7.14) or (7.15) and (7.16) are appropriate for a *simultaneous* QFCT trajectory calculation in which the vibrational part is computed from $\mathbf{P}(t)$ along trajectories for rotationless molecules, and the band contours are computed from $F\{<G_{\beta\gamma}(t)G_{\alpha\delta}(t)>\}$. For our simple normal mode analysis, in Appendix C we evaluate the vibrational correlation function $F\{<P_{\alpha\beta}(0)P_{\gamma\delta}(t)>\}$ in terms of normal coordinate polarizability derivatives. Using those results, we obtain

$$\left(\bar{\lambda}_i\bar{\lambda}_s^3 \frac{d^2\sigma}{d\omega d\Omega}\right)_{iso} = (2\pi)^{-1}\left\{(P^{0,iso})^2\delta(\omega) + \sum_{j=1}^{3}\left(\frac{\partial P^{iso}}{\partial q_j}\right)^2 \frac{\hbar}{2\omega_j}\,\frac{\delta(\omega_j-\omega)}{1-\exp(-\beta\hbar\omega)}\right\} \tag{7.17}$$

$$\left(\bar{\lambda}_i\bar{\lambda}_s^3 \frac{d^2\sigma}{d\omega d\Omega}\right)_{an} = F\{\ <G_{\beta\gamma}(t)G_{\alpha\delta}(t)>\} *$$

$$\left\{P^{0,an}_{\alpha\beta}P^{0,an}_{\gamma\delta}\delta(\omega) + \sum_{j=1}^{3}\frac{\partial P^{an}_{\alpha\beta}}{\partial q_j}\,\frac{\partial P^{an}_{\gamma\delta}}{\partial q_j}\,\frac{\hbar}{2\omega_j}\,\frac{\delta(\omega_j-\omega)}{1-\exp(-\beta\hbar\omega)}\right\}. \tag{7.18}$$

where the superscript 0 indicates the value at the equilibrium position, q_j is the jth normal coordinate, and ω_j is the frequency of the jth normal mode.

Quantum corrections to Raman spectra[2] can be made exactly as for IR spectra (see the discussion at the end of Section VI). Eqs. (7.1) to (7.4) and Eqs. (7.15) and (7.16) can be quantum corrected[2] for rotation and harmonic vibration by Eqs. (6.17) and (6.18), while Eqs. (7.17) and (7.18) require quantum correction only of the rotational motion, using Eq. (6.17).

VIII. SEQUENTIAL INFRARED AND RAMAN APPROACH FOR H_2O

We now compute the infrared band contours for dilute water vapor as an example of an *ab initio sequential* approach using the data from Tables I to III from Sections III and IV and Eqs. (6.1), (6.16), and (6.17) along with the $<G_{\alpha\alpha}(t)>$ elements evaluated as shown in Section V. Rotation is computed classically from the quantum derived equilibrium moments of inertia and vibration is treated quantum mechanically in the normal mode (harmonic) approximation to produce the infrared spectral band contours for the water molecule in the lowest rigid rotor, normal mode approximation. Figure 4 shows the infrared spectral band contours. The upper trace is generated by broadening the water lines from the Air Force Geophysics Laboratory (AFGL) tape[64,65] until they merge into band contours. The AFGL data is derived from experimental measurements with considerable help from theoretical calculations. The lower trace is our simple *ab initio* rigid rotor, normal mode computation of the infrared band contours.

The presence of a Q branch in the infrared spectrum depends upon the value of $F\{<G_{\alpha\alpha}>\}$ at $\omega = 0$. The value of a Fourier transform at $\omega = 0$ depends simply on the integral over all time of the untransformed function. If this area is infinite, then the Fourier transform has a delta function at $\omega = 0$. A delta function in $F<G_{\alpha\alpha}>$ becomes a Q branch when put in Eq. (6.16) if there is a nonzero dipole derivative in the α direction. The area under $<G_{\alpha\alpha}(t)>$ is infinite if

$$\lim_{t\to\infty} <G_{\alpha\alpha}(t)> \neq 0 \,. \tag{8.1}$$

$<G_{\alpha\alpha}(t)>$ can be viewed as the ensemble averaged autocorrelation function of a unit vector fixed in the molecule in the direction of the α principle axis. If rotation about one of the principle axes is very stable, then condition (8.1) can hold, and there will be an infrared Q branch associated with each normal mode that has a dipole derivative component in the direction of that principle axis. In general, rotation about intermediate moments of inertia is very unstable,[59] so that one would not expect[49] any Q branches associated with them. Rotation about the large and the small moments of inertia is generally more stable. Asymptotic formulae for $<G_{\alpha\alpha}(t)>$ are discussed by Guissani, Leicknam, and Bratos.[49] For the case of H_2O, rotation about the smallest moment of inertia, the y axis as shown in Fig. 1, satisfies condition (8.1), as shown in Fig. 3. We obtain a limiting value for that axis of 0.344 and thus the Fourier transform has a delta function of area $2\pi\times 0.344$. Since, as shown in Table III, the ν_3 vibration has a dipole derivative component in the y direction, we obtain a Q branch centered at ν_3. As can be seen from comparing with the experimental spectra in Fig. 4, this rigid rotor central Q branch has an intensity that is too large. We surmise that various effects present in real systems, but not in our ideal rigid rotor, serve to alter the long term behavior of $<G_{yy}(t)>$ and thus the shape of the Q branch in the real spectrum. For instance, the coupling between vibration and rotation or collisions could serve to disturb the ordered rotational effects which lead to condition (8.1). This would allow $<G_{yy}(t)>$ eventually to die off, resulting in a less intense Q branch more in accord with the experimental spectrum. The ν_1 symmetric stretch vibrational rotational band is very small in comparison with the ν_3 band, and is hardly seen. The ν_2 symmetric bend band has no Q branch because its non-zero dipole moment derivative is along the intermediate moment of inertia axis and rotation about this axis is unstable. The difference between the theoretical and experimental ratios of the P and R type branches in the ν_2 band is at the moment unexplained. For a different approach, in which an *ab initio* dipole moment function is used to compute the strengths of vibration - rotation lines see the work of Carney.[66]

Figure 5 shows the isotropic and anisotropic rigid rotor, normal mode Raman spectral band contours of dilute water vapor as given by our *ab initio* calculations, using the data from Tables I-III and Eqs. (7.17), (7.18), and (6.17) with the elements of $<G_{\beta\gamma}(t)G_{\alpha\delta}(t)>$ computed as shown in Section V. Note that in our computed Raman spectra, the OH stretching region has strong contributions from both the totally symmetric stretch ν_1 and the asymmetric stretch ν_3, as is seen experimentally,[46] while the infrared stretching region is dominated by the asymmetric stretch ν_3. The results for the isotropic case from our calculations are actually delta

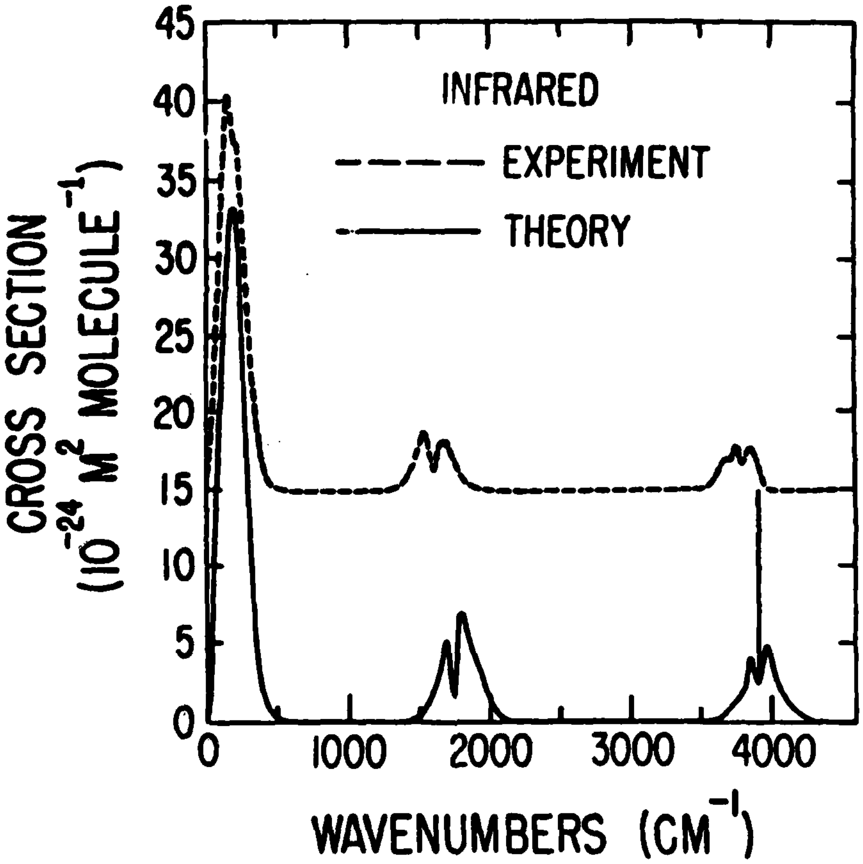

Figure 4. Comparison of measured and computed infrared spectral band contours for H_2O vapor at 296 K. The "experimental" spectrum is derived by broadening the spectral lines from the Air Force Geophysics Laboratory tape, and is plotted with its baseline raised by 15×10^{-24} m^2 $molecule^{-1}$ for clarity. The *ab initio sequential* theoretical spectrum is computed in the rigid rotor, normal mode approximation using quantum mechanical normal mode vibration with a classical calculation (from the quantum derived equilibrium moments of inertia) of the band shapes arising from rotational motion. The left and tallest peak is pure rotation, the middle peaks at approximately 1500 to 2000 cm^{-1} are the ν_2 bending mode and the peaks on the right at approximately 3500 to 4500 cm^{-1} are the OH stretching, the ν_1 symmetric stretch being so weak as to be hardly seen and the ν_3 asymmetric stretch thus dominating the stretching region. The sharp peak in the stretching region of the theoretical spectrum is the ν_3 Q branch, which can be seen to be much broader and weaker in the experimental spectrum, indicating that the real long term vectorial correlation dies off more quickly than the rigid rotor one. Note that the theoretical vibrational rotational peaks occur at higher frequencies than the experimental ones because anharmonicity was not included in this normal mode calculation.

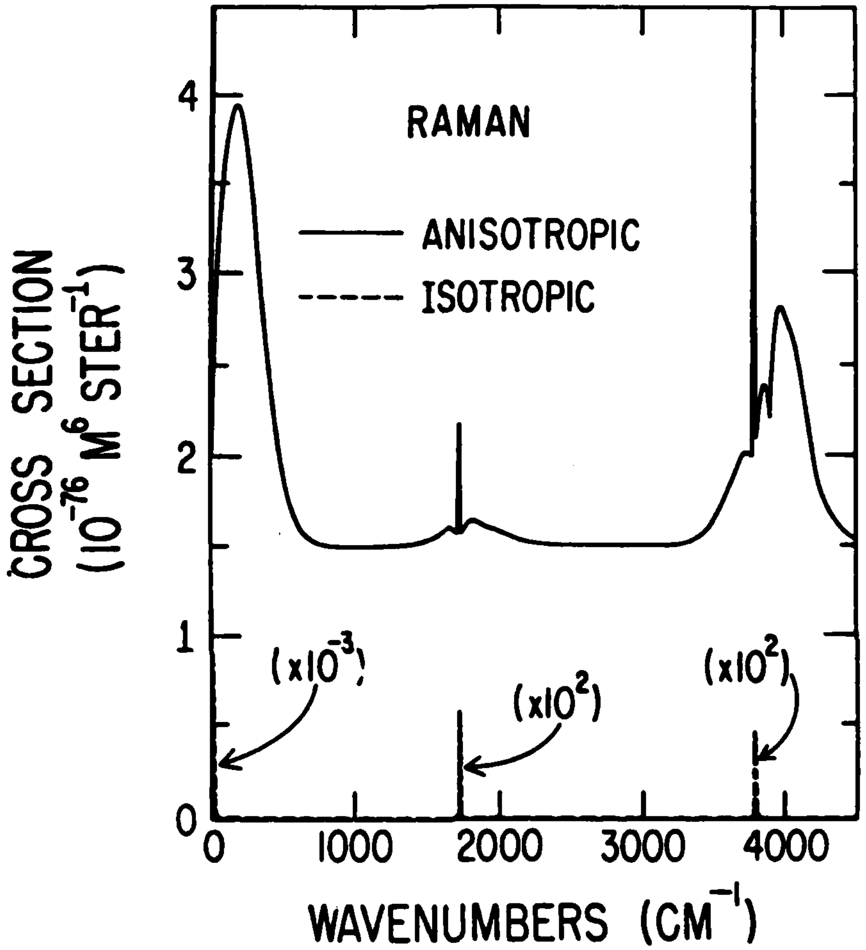

Figure 5. *Ab initio sequential* isotropic and anisotropic Raman spectral band contours for H_2O vapor. The spectra are computed in the rigid rotor, normal mode approximation using quantum mechanical normal mode vibration with a classical rotational calculation of the band contours from the quantum equilibrium moments of inertia. The temperature is 296 K. The overall band contour in the Raman OH stretch region, 3500 to 4500 cm^{-1}, has significant contributions from both the symmetric stretch ν_1 and the asymmetric stretch ν_3, in contrast to the infrared OH stretch region, which is dominated by ν_3. The sharp Q branch peak in the Raman stretching region is due to ν_1, while that for the infrared region is due to ν_3. Due to space limitations, the heights of the anisotropic Q branches for pure rotation and for ν_1 are cut off at the upper margin of the figure. The anisotropic spectrum is plotted with a vertical offset of 1.5×10^{-76} m^2ster^{-1}, in which *ster* means steradians. Note that the experimental vibrational rotational bands will be somewhat lower in frequency than the normal mode frequencies shown here due to vibrational anharmonicity.

functions at 0, ν_1, and ν_2. There is nothing for ν_3 in the isotropic spectrum because the corresponding isotropic polarizability derivatives along the diagonal in Table III are zero. We have broadened the delta functions so as to be able to present them graphically. Although experimental Raman line spectra of water vapor have been measured,[46-48, 67, 68] the available experimental band contours [67] are of low signal to noise ratio and make accurate comparison with our calculations difficult. Water vapor pressurized by an inert gas could provide lines appropriately broadened and merged into a band contour for an experimental comparison with this calculation. A comparison with quantum theory could be made by broadening the line spectrum from an accurate quantum calculation.[47, 48]

Several points can, however, be deduced from the available Raman band contour and line spectral data.[46-48, 67, 68] As is also seen experimentally,[48, 67] our pure rotational anisotropic band at approximately 0 to 500 cm^{-1} is indeed much weaker than the corresponding pure rotational band[2] for N_2. Our computed equilibrium polarizability matrix elements given in Table II, which produce the rotational spectrum, compare quite well with those deduced experimentally by Murphy,[48] when his axis convention is converted to ours[42] by $x \rightarrow z$, $y \rightarrow x$, $z \rightarrow y$. The computed ν_2 bending band at approximately 1500 to 2000 cm^{-1} is indeed much weaker than the OH stretch region, as is found experimentally,[47, 67] and, as well as we can judge from the published figures, the computed ν_2 band shape at least qualitatively resembles that of the observed line spectrum,[47] except that our ν_2 Q branch appears somewhat sharper than the experimental one. The computed OH stretch region (the 3500 to 4500 cm^{-1} band) also resembles the available survey band spectrum of Penney and Lapp[67] and, as well as we can judge from the published figures, also resembles the line spectrum measured by Murphy.[46] In Murphy's line spectrum[46] we see the strong ν_1 Q branch as in our spectrum (although the experimental Q branch is broader), as well as the major contribution from ν_3 with no Q branch as we also observe in our calculation.

Note that the computed infrared and Raman vibrational rotational bands are at higher frequencies than the experimental ones because only the harmonic forces were used in this simple normal mode calculation, and the anharmonicity which we did not compute lowers the real frequencies.

IX. SIMULTANEOUS QUANTUM FORCE CLASSICAL TRAJECTORY APPROACH

In addition to the *sequential* approach illustrated in the H_2O example presented in Section VIII above, a *simultaneous* quantum force classical trajectory (QFCT) approach can also be taken which is likely to be more practical for many atom systems. Given the force $\mathbf{F}_i$ on each atom i at position $\mathbf{r}_i$ from the quantum gradient technique described in Section III, we can in principle integrate forward one step in time the classical equations of motion

$$\mathbf{F}_i = m_i \frac{d^2\mathbf{r}_i}{dt^2}\ , \quad i = 1, \ldots, N \tag{9.1}$$

for the N atoms. (For nearly harmonic systems such as isolated molecules, the trigonometric polynomial fitting routine of Gautschi[69] may be of interest.) Then, given the new set of positions, we can derive from the quantum part of our calculation new values of the $\mathbf{F}_i$, and of whatever quantities such as $\boldsymbol{\mu}$ (for the infrared spectrum), and $\mathbf{P}$ (for the Raman spectrum) we wish in addition.

From an ensemble of the time histories $\boldsymbol{\mu}(t)$ and $\mathbf{P}(t)$, we can derive the infrared[1] and Raman[2] spectra, using Eqs. (6.1) to (6.5) and (7.1) to (7.4), in either the correlation function or power spectrum forms. The appropriate simple quantum corrections shown in Eqs. (6.17) and (6.18) are discussed in other papers.[1, 2, 14] As illustrated elsewhere, these techniques can be extended to calculate the infrared and Raman spectra of non-equilibrium and time dependent systems,[14, 70] as well as the electronic absorption spectra of equilibrium and non-equilibrium systems.[71]

Because the computational demands of a many atom *simultaneous* approach are high, careful thought is warranted as to how to efficiently average over the ensemble of interest. For an equilibrium ensemble, we can start a series of runs by approximating the initial phase space distribution in the following manner. If the system in question were completely harmonic, on the average its total internal energy would be equally divided into kinetic and potential energy. If we start our atoms at the equilibrium positions, but give them velocities chosen randomly from a Boltzmann distribution corresponding to twice the temperature, we would give the molecule the correct distribution of total energy for the true temperature if it were truly harmonic. One could remove angular momentum by adding on a rotational term to the velocities corresponding to a coordinate system rotating in the opposite direction to the initial angular velocity, and then rechoose a rotational angular momentum for the system corresponding to the real temperature of interest. For an anharmonic system this is only an approximation; in addition, starting each run at the equilibrium position for even a multidimensional harmonic oscillator may not sample all of phase space. One therefore would use this method only for the first equilibration run. For each run thereafter, one would use the final positions in the previous run as initial positions, and give a new set of random initial velocities chosen from the Boltzmann distribution corresponding to the true temperature. After a number of such runs, the system would be equilibrated at the desired temperature, and one could begin to take data.

An advantage of the *simultaneous* QFCT *ab initio* molecular dynamic approach described above is its simplicity. No separation of translational, rotational, and vibrational motion and no normal mode approximations are needed. The computation may equally well be carried out for gases of individual molecules, clusters, liquids, solutions, or solids. Many other measurables besides infrared, Raman, and electronic spectra may also be computed in a parallel QFCT manner, by quantum mechanically calculating parameters along the trajectory and then performing the appropriate averages over an ensemble of trajectories. For example, thermodynamic variables such as energy, heat capacity, free energy, and entropy can be computed in a QFCT manner from quantum evaluation of the potential energy seen by the nuclei and classical evaluation of the nuclear kinetic energy with averaging over proper ensembles of trajectories.[19] In addition, by keeping track of velocities along the classical paths and power spectral transformation to velocity spectra, the quantum corrections to these thermodynamic variables may also be computed.[19]

In cases in which the above approach is too demanding in terms of available computer power, again, as in the *sequential* case, a rigid rotor vibrator approximation can be made and the effect of the rotational motions handled entirely classically once the quantum equilibrium geometry is known. For example, to compute infrared spectra in this way one would use Eqs. (6.1), (6.12) to (6.15), (6.17) and (6.18) and to compute Raman spectra Eqs. (7.11) to (7.16), (6.17) and (6.18), choosing either the convolution or power spectral methods.

X. DISCUSSION AND CONCLUSION

We have shown that a judicious combination of quantum mechanics and classical mechanics can be used to compute *ab initio* infrared and Raman spectral band contours. Two different approaches are discussed. In the first, one *sequentially* solves the electronic and then the nuclear parts of the Born-Oppenheimer approximation, and in the second they are solved *simultaneously*. We have presented an example at the simplest rigid rotor, normal mode level for the *sequential* approach. The accuracy of this simplest approach is not exceptional, but it could certainly be considerably improved by bringing in effects beyond the rigid rotor, normal mode level such as centrifugal distortion, vibration rotation interaction (for example Coriolis effects) and anharmonic effects. In addition, the effects of terms beyond the linear expansion for the dipole moment and polarizability tensor could be considered.

In developing the methodology for the *sequential* rigid rotor, normal mode approach, we have worked out an improved, simple, accurate, and fast technique to compute pure rotational and vibrational - rotational classical rigid rotor infrared and Raman band contours for any molecule, including asymmetric tops. Comparison with the pioneering work on asymmetric rotors by Leicknam, Guissani, and Bratos[49-56] shows agreement at intermediate and higher displacements from the band center, but some quantitative disagreement nearer the band centers where we believe we were able to achieve higher accuracy. The overall qualitative picture is the same, but we achieve it with a simple and rapid calculation which avoids complexities such as reference to Euler angles and special functions.

We discuss a second *simultaneous* approach, which we call Quantum Force Classical Trajectory (QFCT), which is more appropriate for many atom systems such as large molecules, clusters, and liquids. In this latter approach, which closely follows the spirit of our earlier molecular dynamics approaches to infrared[1] and Raman[2] spectra, there is no need to separate vibrational, rotational, and translational motion or to make normal mode approximations. The generality of the approach is such that it can in principle be applied to gas, liquid or solid systems, composed of stable or unstable species, in equilibrium or not.[14] The QFCT method could also be employed to compute other spectral (for example electronic absorption[71]) and transport properties derivable from correlation functions, to deduce thermodynamic quantities,[19] and to study chemical reactions, as has already been demonstrated by Warshel and Karplus[12] and by Leforestier.[13] A parallel Monte Carlo approach in which energies are computed quantum mechanically at each trial step and other measurables computed at the accepted steps might be used in the computation of parameters which do not depend on momenta.

ACKNOWLEDGEMENTS

We thank the National Aeronautics and Space Administration, Ames Research Center, the Office of Naval Research, Chemistry, the National Science Foundation, Chemistry, and the National Institutes of Health, Division of Research Resources, for providing the support which has made this work possible. A.K. has been supported by a grant, NCC2-154, from the National Aeronautics and Space Administration, Ames Research Center. In addition, we thank Peter H. Berens, Donald H. J. Mackay, and Gary M. White whose work on related theoretical problems has greatly contributed to this paper.

APPENDIX A

In the classical statistical mechanics of a rigid body, we are required to calculate equilibrium averages by integration over phase space, using the canonical volume element $d\Gamma = dq^1 dq^2 dq^3 dp_1 dp_2 dp_3$, where $q^\sigma (\sigma = 1,2,3)$ are coordinates in the rotation group (eg., Euler angles) and p_σ are the canonically conjugate momenta. In practice, it is often easier to use the volume element $dV\, dl_1 dl_2 dl_3$, where l_μ $(\mu = 1,2,3)$ are the components of the angular momentum in the body frame, related to the angular velocity by $l_\mu = I_{\mu\nu}\omega_\nu$ ($I_{\mu\nu}$ is the moment of inertia tensor in the body frame and we again in this appendix use the summation notation), and dV is the invariant volume element in the rotation group. We have not found an adequate reference for this procedure, so we justify it here.

The connection between q and ω is given by the rotation matrix $D_{i\alpha}(q)$ [see Eq. (5.7)]

$$\dot{D}_{i\alpha} = \frac{\partial D_{i\alpha}(q)}{\partial q^\sigma}\, \dot{q}^\sigma = \omega_\mu \epsilon_{\beta\mu\alpha} D_{i\beta}(q) \, , \tag{A1}$$

so that the angular velocity ω in the body frame, is related to the configurational velocity $\dot{q}$ by

$$\omega_\mu = \tfrac{1}{2}\epsilon_{\beta\mu\alpha} D_{i\beta}(q) \frac{\partial D_{i\alpha}(q)}{\partial q^\sigma}\, \dot{q}^\sigma = A_{\mu\sigma}(q)\dot{q} \, . \tag{A2}$$

(The second equality defines the matrix A.) The Lagrangian is

$$L = \tfrac{1}{2} I_{\mu\nu}\omega_\mu\omega_\nu \, , \tag{A3}$$

so the canonical momenta are

$$p_\sigma = \frac{\partial L}{\partial q^\sigma} = I_{\mu\nu}\omega_\mu \frac{\partial \omega_\nu}{\partial \dot{q}^\sigma} = I_{\mu\nu}\omega_\mu A_{\nu\sigma} = l_\nu A_{\nu\sigma}. \tag{A4}$$

The canonical phase space volume element is

$$d\Gamma = dq^1 dq^2 dq^3 (\det A)\, dl_1 dl_2 dl_3$$

$$= dV\, dl_1 dl_2 dl_3 \tag{A5}$$

with $dV = (\det A)dq^1 dq^2 dq^3$, which, we claim, is the invariant volume element in the rotation group.

Define the differential forms $\lambda_\nu = A_{\nu\sigma} dq^\sigma$, so that $dV = \lambda_1 \lambda_2 \lambda_3$ (exterior product). The forms λ_ν are left invariant:

$$\lambda_\nu = A_{\nu\sigma} dq^\sigma = \tfrac{1}{2}\epsilon_{\beta\nu\alpha} D_{i\beta}(q) \frac{\partial D_{i\alpha}(q)}{\partial q^\sigma} dq^\sigma = \tfrac{1}{2}\epsilon_{\beta\nu\alpha} D_{i\beta}(q)\, dD_{i\alpha}(q). \tag{A6}$$

For fixed r,

$$\lambda_\nu(rq) = \tfrac{1}{2}\epsilon_{\beta\nu\alpha} D_{i\beta}(rq)\, dD_{i\alpha}(rq)$$

$$= \tfrac{1}{2}\epsilon_{\beta\nu\alpha} D_{ij}(r) D_{j\beta}(q) D_{ik}(r)\, dD_{k\alpha}(q) \tag{A7}$$

$$= \tfrac{1}{2}\epsilon_{\beta\nu\alpha} D_{i\beta}(q)\, dD_{i\alpha}(q) = \lambda_\nu(q) \ , \tag{A8}$$

where we use the orthogonality of $D_{ik}(r)$. Since the λ_ν are left invariant, so is their exterior product dV.

The probability distribution in phase space is $d\Gamma \exp(-\beta H)$, where H is the Hamiltonian. We have

$$H = \tfrac{1}{2} I^{-1}_{\mu\nu} l_\mu l_\nu = \tfrac{1}{2} I_{\mu\nu} \omega_\mu \omega_\nu \ , \tag{A9}$$

and

$$d\Gamma = dV\, dl_1 dl_2 dl_3 = \det(I)\, dV\, d\omega_1 d\omega_2 d\omega_3 \ , \tag{A10}$$

so the averaging procedure of Eq. (5.10) has been justified.

APPENDIX B: SYMMETRY IN THE INERTIA TENSOR

We can take advantage of symmetry in the molecule's inertia tensor to show that most of the elements and products of <G> are zero. Consider a rotation **R** which commutes with the inertia tensor **I**, so that **IR** = **RI** . We will now show that if $\boldsymbol{\omega}(t,\boldsymbol{\omega}^0)$ satisfies the equations of motion, then so does $\mathbf{R}\boldsymbol{\omega}(t,\boldsymbol{\omega}^0)$. We have, using the summation notation,

$$I_{\alpha\beta} \frac{d}{dt}(\mathbf{R}\boldsymbol{\omega})_\beta = I_{\alpha\beta} R_{\beta\mu} \frac{d\omega_\mu}{dt} \tag{B1}$$

$$= R_{\alpha\beta} I_{\beta\mu} \frac{d\omega_\mu}{dt} \tag{B2}$$

$$= -R_{\alpha\beta} I_{\gamma\mu} \omega_\mu \omega_\nu \epsilon_{\nu\gamma\beta} \ , \tag{B3}$$

in which $\epsilon_{\nu\gamma\beta}$ is again the Levi-Civita density. Since **R** is orthogonal, $R_{\sigma\nu} R_{\sigma\nu'} = \delta_{\nu\nu'}$ and $R_{\tau\gamma} R_{\tau\gamma'} = \delta_{\gamma\gamma'}$, so we can write

$$I_{\alpha\beta} \frac{d}{dt}(\mathbf{R}\boldsymbol{\omega})_\beta = -R_{\alpha\beta} \delta_{\nu\nu'} \delta_{\gamma\gamma'} \epsilon_{\nu'\gamma'\beta} I_{\gamma\mu} \omega_\mu \omega_\nu \tag{B4}$$

$$= -R_{\alpha\beta} R_{\sigma\nu} R_{\sigma\nu'} R_{\tau\gamma} R_{\tau\gamma'} \epsilon_{\nu'\gamma'\beta} I_{\gamma\mu} \omega_\mu \omega_\nu \ . \tag{B5}$$

Using the definition of a determinant and the fact that **R** is orthogonal one can show that

$$R_{\alpha\beta} R_{\sigma\nu'} R_{\tau\gamma'} \epsilon_{\nu'\gamma'\beta} = \epsilon_{\alpha\sigma\tau} \det \mathbf{R} = \epsilon_{\alpha\sigma\tau} \ , \tag{B6}$$

where det is the determinant. This leads to

$$I_{\alpha\beta} \frac{d}{dt}(\mathbf{R}\boldsymbol{\omega})_\beta = -R_{\sigma\nu} R_{\tau\gamma} \epsilon_{\alpha\sigma\tau} I_{\gamma\mu} \omega_\mu \omega_\nu \tag{B7}$$

$$= -\epsilon_{\alpha\sigma\tau} I_{\tau\gamma} (\mathbf{R}\boldsymbol{\omega})_\gamma (\mathbf{R}\boldsymbol{\omega})_\sigma \tag{B8}$$

which is just Eq. (5.5) with $\mathbf{R}\boldsymbol{\omega}$ in place of $\boldsymbol{\omega}$. Because $\boldsymbol{\omega}(t,\mathbf{R}\boldsymbol{\omega}^0)$ and $\mathbf{R}\boldsymbol{\omega}(t,\boldsymbol{\omega}^0)$ satisfy the same equations of motion and have the same initial conditions, they must be equal, so that $\boldsymbol{\omega}(t,\mathbf{R}\boldsymbol{\omega}^0) = \mathbf{R}\boldsymbol{\omega}(t,\boldsymbol{\omega}^0)$.

We will now show that if the set $\mathbf{D}(t),\boldsymbol{\omega}(t)$ satisfies the equations of motion, then so does $\mathbf{D}(t)\mathbf{R}^{-1},\mathbf{R}\boldsymbol{\omega}(t)$. Putting $\mathbf{D}(t)\mathbf{R}^{-1}$ into Eq. (5.7), we have

$$\frac{d}{dt}(\mathbf{D}\mathbf{R}^{-1})_{i\alpha} = \omega_\beta \epsilon_{\beta\mu\gamma} D_{i\gamma} R_{\alpha\mu} \tag{B9}$$

$$= R_{\sigma\beta'} R_{\alpha\mu} R_{\tau\gamma'} \epsilon_{\beta'\mu\gamma'} R_{\sigma\beta} R_{\tau\gamma} \omega_\beta D_{i\gamma} \tag{B10}$$

$$= \epsilon_{\sigma\alpha\tau} R_{\sigma\beta} \omega_\beta D_{i\gamma} R_{\tau\gamma} \tag{B11}$$

$$= \epsilon_{\sigma\alpha\tau} \, (\mathbf{R}\boldsymbol{\omega})_\sigma (\mathbf{D}\mathbf{R}^{-1})_{i\tau} \; . \tag{B12}$$

For any given solution of Eqs. (5.6), the solution of Eq. (5.7) is unique, for given initial conditions. When we are dealing with $\mathbf{G}$, however, the initial conditions are always the same: $\mathbf{G}(0,\boldsymbol{\omega}^0) = \mathbf{1}$. By definition, $\mathbf{G}(t,\mathbf{R}\boldsymbol{\omega}^0)$ is a solution to Eq. (5.7) given that the solution to Eqs. (5.6) is $\mathbf{R}\boldsymbol{\omega}^0$. Similarly, we have just obtained that $\mathbf{D}(t)\mathbf{R}^{-1}$ is a solution subject to the same solution for $\boldsymbol{\omega}$. The initial conditions do not match however, but since $\mathbf{D}(t)\mathbf{R}^{-1}$ is a solution, by the isotropy of space, so is $\mathbf{R}\mathbf{D}(t)\mathbf{R}^{-1}$, which matches initial conditions. This implies that

$$\mathbf{G}(t,\mathbf{R}\boldsymbol{\omega}^0) = \mathbf{R}\mathbf{G}(t,\boldsymbol{\omega}^0)\mathbf{R}^{-1} \; . \tag{B13}$$

For the infrared case [49-56] we can use Eq. (B13) to show that $<\mathbf{G}(t)>$ is diagonal. $\mathbf{I}$ in the body frame commutes with each of the following 180° rotations:

$$\sigma_x = \begin{bmatrix} 1 & 0 & 0 \\ 0 & -1 & 0 \\ 0 & 0 & -1 \end{bmatrix} ; \; \sigma_y = \begin{bmatrix} -1 & 0 & 0 \\ 0 & 1 & 0 \\ 0 & 0 & -1 \end{bmatrix} ; \; \sigma_z = \begin{bmatrix} -1 & 0 & 0 \\ 0 & -1 & 0 \\ 0 & 0 & 1 \end{bmatrix} . \tag{B14}$$

For any off diagonal element of $\mathbf{G}$, $G_{\alpha\beta}$ with $\alpha \neq \beta$, $(\sigma_\alpha \mathbf{G} \sigma_\alpha^{-1})_{\alpha\beta} = -G_{\alpha\beta}$ (no summation), so putting this into Eq. (B13)

$$G_{\alpha\beta}(t,\sigma_\alpha\boldsymbol{\omega}^0) = -G_{\alpha\beta}(t,\boldsymbol{\omega}^0) \; . \tag{B15}$$

For a Boltzmann distribution of angular velocities equal weight is given to $\boldsymbol{\omega}$ and $\sigma_\alpha\boldsymbol{\omega}$, so

$$< G_{\alpha\beta}(t) > = -< G_{\alpha\beta}(t) > = 0, \quad \alpha \neq \beta \; , \tag{B16}$$

and we conclude that $<\mathbf{G}(t)>$ is diagonal.

In order to calculate Raman spectra we need to calculate $< G_{\alpha\beta} G_{\gamma\delta} >$. If some one of $\{\alpha,\beta,\gamma,\delta\}$ is unique, say β (i.e., $\beta \neq \gamma$, $\beta \neq \alpha$, and $\beta \neq \delta$), then application of σ_β as above will change the sign of $G_{\alpha\beta} G_{\gamma\delta}$ and we will get $< G_{\alpha\beta} G_{\gamma\delta} > = 0$. Therefore the indices must come in pairs, and the nonzero elements are of the form $< G_{\alpha\beta}^2 >$, $< G_{\alpha\beta} G_{\beta\alpha} >$, or $< G_{\alpha\alpha} G_{\beta\beta} >$.

Because with the application of each of the rotations in Eq. (B14) one can generate the entire sphere from any two adjacent octants, and one need only do the averaging over the sphere for two adjacent octants.

APPENDIX C: DERIVATION OF THE VIBRATIONAL CORRELATION FUNCTIONS

Given two observables A and B, we wish to evaluate

$$F\{< A(0) B(t) >\} \tag{C1}$$

in terms of normal coordinates. In this appendix we will not use the summation notation. For the infrared case we take $A = B = \mu_\alpha$, and for the Raman case $A = P_{\alpha\beta}$ and $B = P_{\gamma\delta}$. We approximate A and B in a Taylor's series in terms of normal coordinates q_j, keeping only terms to first order, obtaining

$$A(0) = A^0 + \Delta A = A^0 + \sum_j \frac{\partial A}{\partial q_j} q_j(0) \tag{C2}$$

and

$$B(t) = B^0 + \Delta B(t) = B^0 + \sum_j \frac{\partial B}{\partial q_j} q_j(t) \tag{C3}$$

where A^0 and B^0 denote the values of A and B at equilibrium, and the derivatives are evaluated at equilibrium.

From the fluctuation-dissipation theorem[18] and the Kubo formula,[18] we have

$$F\{<A(0)B(t)>\} = 2\pi\delta(\omega)A^0B^0 + \frac{1}{1-\exp(-\beta\hbar\omega)} F\{<[\Delta A(0),\Delta B(t)]>\} , \tag{C4}$$

where [] denotes commutation. Using (C2) and (C3) we can write

$$[\Delta A(0),\Delta B(t)] = \sum_{j,k} \frac{\partial A}{\partial q_j} \frac{\partial B}{\partial q_k} [q_j(0),q_k(t)] . \tag{C5}$$

In the harmonic approximation, $q_k(t)$ in the Heisenberg representation is the same as the classical solution for a simple harmonic oscillator

$$q_k(t) = q_k(0)\cos\omega_k t + \frac{p_k(0)}{\omega_k} \sin\omega_k t , \tag{C6}$$

where p_k is the momentum corresponding to the kth normal mode. Using this, we obtain

$$[q_j(0),q_k(t)] = \delta_{jk} \frac{i\hbar}{\omega_k} \sin\omega_k t . \tag{C7}$$

Putting this back in Eq. (C4), and using the relations

$$\sin\omega_k t = \frac{e^{i\omega_k t} - e^{-i\omega_k t}}{2i} \tag{C8}$$

and

$$2\pi\delta(\omega) = \int_{-\infty}^{\infty} e^{-i\omega t} dt , \tag{C9}$$

we obtain

$$F\{<A(0)B(t)>\} = 2\pi\Big\{\delta(\omega)A^0B^0$$

$$+ \frac{1}{1-\exp(-\beta\hbar\omega)} \sum_j \frac{\hbar}{2\omega_j} \frac{\partial A}{\partial q_j} \frac{\partial B}{\partial q_j} [\delta(\omega-\omega_j) - \delta(\omega+\omega_j)]\Big\} . \tag{C10}$$

For the infrared case, we then have

$$F\{<\mu_\alpha(0)\mu_\alpha(t)>\} = 2\pi\Big\{\delta(\omega)\big(\mu_\alpha^0\big)^2$$

$$+ \frac{1}{1-\exp(-\beta\hbar\omega)} \sum_j \frac{\hbar}{2\omega_j} (\frac{\partial\mu_\alpha}{\partial q_j})^2 [\delta(\omega-\omega_j) - \delta(\omega+\omega_j)]\Big\} , \tag{C11}$$

where μ_α^0 is the α component of the equilibrium dipole moment, and ω_j is the angular frequency of the jth normal mode.

For the Raman case we have

$$F\{<P_{\alpha\beta}(0)P_{\gamma\delta}(t)>\} = 2\pi\Big\{\delta(\omega)P_{\alpha\beta}^0 P_{\gamma\delta}^0$$

$$+ \frac{1}{1-\exp(-\beta\hbar\omega)} \sum_j \frac{\hbar}{2\omega_j} \frac{\partial P_{\alpha\beta}}{\partial q_j} \frac{\partial P_{\gamma\delta}}{\partial q_j} [\delta(\omega-\omega_j) - \delta(\omega+\omega_j)]\Big\} , \tag{C12}$$

where $P_{\alpha\beta}^0$ is the $\alpha\beta$ component of the equilibrium polarizability tensor.

In both cases, the delta functions centered at $-\omega_j$ play no role in our calculations because the rotational spectrum is very narrow compared to ω_j.

References

1. P. H. Berens and K. R. Wilson, *J. Chem. Phys.* 74, 4872 (1981).
2. P. H. Berens, S. R. White, and K. R. Wilson, *J. Chem. Phys.* 75, 515 (1981).
3. H. C. Allen, Jr. and P. C. Cross, *Molecular Vib-Rotors* (John Wiley, New York, 1963).
4. W. F. Murphy, *J. Raman. Spectrosc.* 11, 339 (1981).
5. E. B. Wilson, Jr., J. C. Decius, and P. C. Cross, *Molecular Vibrations* (McGraw-Hill, New York, 1955).
6. S. Califano, *Vibrational States* (Wiley, London, 1976).
7. D. F. Coker, J. R. Reimers, and R. O. Watts, *Aust. J. Phys.*, in press.
8. E. N. Svendsen and J. Oddershede, *J. Chem. Phys.* 71, 3000 (1979).
9. M. L. Koszykowski, D. W. Noid, and R. A. Marcus, *J. Phys. Chem.* 86, 2113 (1982).
10. E. J. Heller, *Accts. Chem. Res.* 14, 368 (1981).
11. K. R. Wilson, in *Minicomputers and Large Scale Computations*, edited by P. Lykos (American Chemical Society, Washington, 1977) p. 147.
12. A. Warshel and M. Karplus, *Chem. Phys. Lett.* 32, 11 (1975).
13. C. Leforestier, *J. Chem. Phys.* 68, 4406 (1978).
14. P. H. Berens, J. P. Bergsma, and K. R. Wilson, to be submitted.
15. R. Zwanzig, *Annu. Rev. Phys. Chem.* 16, 67 (1965).
16. R. G. Gordon, *Adv. Magn. Reson.* 3, 1 (1968).
17. B. J. Berne, in *Physical Chemistry, An Advanced Treatise*, edited by D. Henderson (Academic Press, New York, 1971) Vol. VIIIB, Chap. 9.
18. D. A. McQuarrie, *Statistical Mechanics* (Harper and Row, New York, 1976).
19. P. H. Berens, D. H. J. Mackay, G. M. White, and K. R. Wilson, *J. Chem. Phys.*, submitted.
20. P. J. Rossky, J. D. Doll, and H. L. Friedman, *J. Chem. Phys.* 69, 4628 (1978).
21. C. Pangali, M. Rao, and B. J. Berne, *Chem. Phys. Lett.* 55, 413 (1978).
22. M. Rao, C. Pangali, and B. J. Berne, *Mol. Phys.* 37, 1773 (1979).
23. A. Komornicki, K. Ishida, K. Morokuma, R. Ditchfield, and M. Conrad, *Chem. Phys. Lett.* 45, 595 (1977).
24. J.W. McIver, Jr. and A. Komornicki, *Chem. Phys. Lett.* 10, 303 (1971).
25. J.W. McIver, Jr. and A. Komornicki, *J. Am. Chem. Soc.* 94, 2625 (1972).
26. A. Komornicki and J.W. McIver, Jr., *J. Am. Chem. Soc.* 95, 4512 (1973).
27. A. Komornicki and J.W. McIver, Jr., *J. Am. Chem. Soc.* 96, 5798 (1974).
28. P. Pulay, in *Methods of Electronic Structure Theory*, edited by H.F. Schaefer III (Plenum Press, New York, 1977) p. 153.
29. A. Komornicki, J.D. Goddard, and H.F. Schaefer III, *J. Am. Chem. Soc.* 102, 1763 (1980).
30. A. Komornicki, C.E. Dykstra, M.A. Vincent, and L. Radom, *J. Am. Chem. Soc.* 103, 1652 (1981).
31. A. Komornicki and J.W. McIver, Jr., *J. Chem. Phys.* 70, 2014 (1979).
32. A. Komornicki and R.L. Jaffe, *J. Chem. Phys.* 71, 2150 (1979).
33. W. B. Person, K. G. Brown, D. Steele, and D. Peters, *J. Phys. Chem.* 85, 1998 (1981).

34. D. Steele, W. B. Person, and K. G. Brown, *J. Phys. Chem.* **85**, 2007 (1981).

35. GRADSCF is an *ab initio* gradient program system designed and written by A. Komornicki at Polyatomics Research, and supported on grants and contracts through NASA Ames Research Center. A version dated January 1979 of this program is available through the QCPE program exchange at the University of Indiana..

36. S. Bratoz, *Colloq. Int. C.N.R.S.* **82**, 287 (1958).

37. R. Moccia, *Theor. Chim. Acta* **8**, 8 (1967).

38. J. Gerratt and I.M. Mills, *J. Chem. Phys.* **49**, 1719 (1968).

39. P. Pulay, *Mol. Phys.* **17**, 197 (1969).

40. M. Dupuis, *J. Chem. Phys.* **74**, 5758 (1981).

41. B.A. Murtaugh and R.W. Sargent, *Comput. J.* **13**, 188 (1978).

42. Joint Commission for Spectroscopy of the International Astronomical Union and the International Union of Pure and Applied Physics, *J. Chem. Phys.* **23**, 1997 (1955).

43. P.C. Hariharan and J.A. Pople, *Mol. Phys.* **27**, 209 (1974).

44. T.H. Dunning, Jr., *J. Chem. Phys.* **55**, 716 (1971).

45. C. Camy-Peyret and J.-M. Flaud, *Mol. Phys.* **32**, 523 (1976).

46. W.F. Murphy, *Mol. Phys.* **36**, 727 (1978).

47. W.F. Murphy, *Mol. Phys.* **33**, 1701 (1977).

48. W.F. Murphy, *J. Chem. Phys.* **67**, 5877 (1977).

49. Y. Guissani, J.C. Leicknam, and S. Bratos, *Phys. Rev. A* **16**, 2072 (1977).

50. S. Bratos, J.C. Leicknam, and Y. Guissani, *J. Mol. Struct.* **47**, 15 (1978).

51. J.C. Leicknam, Y. Guissani, and S. Bratos, *J. Chem. Phys.* **68**, 3380 (1978).

52. J.C. Leicknam, Y. Guissani, and S. Bratos, *Phys. Rev. A* **21**, 1005 (1980).

53. J-Cl. Leicknam, *Phys. Rev. A* **22**, 2286 (1980).

54. Y. Guissani and J-Cl. Leicknam, *J. Chem. Phys.* **75**, 2066 (1981).

55. J-Cl. Leicknam and Y. Guissani, *Mol. Phys.* **42**, 1105 (1981).

56. J-Cl. Leicknam and Y. Guissani, *J. Mol. Struct.* **80**, 377 (1982).

57. A. G. St. Pierre and W. A. Steele, *Phys. Rev.* **184**, 172 (1969).

58. VAX is a trademark of Digital Equipment Corp..

59. H. Goldstein, *Classical Mechanics* (Addison-Wesley Pub. Co., 1980).

60. K. Atkinson, *J. Aust. Math. Soc.(Series B)* **23**, 332 (1982).

61. C. W. Gear, *Numerical Initial Value Problems in Ordinary Differential Equations* (Prentice-Hall, Englewood Cliffs, 1971).

62. G. A. Korn and T. M. Korn, *Mathematical Handbook for Scientists and Engineers* (McGraw-Hill Book Company, New York, 1961) p. 580.

63. E. J. Heller, R. L. Sundberg, and D. Tannor, *J. Phys. Chem.* **86**, 1822 (1982).

64. L. S. Rothman, *Appl. Opt.* **20**, 791 (1981).

65. R. A. McClatchey, W. S. Benedict, S. A. Clough, D. E. Burch, R. F. Calfee, K. Fox, L. S. Rothman, and J. S. Garing, "AFCRL atmospheric absorption line parameters compilation," AFCRL-TR-73-0096, Air Force Cambridge Research Laboratories, L. G. Hanscom Field, Bedford, Massachusetts (1973).

66. G. D. Carney, *Appl. Spectrosc.* **33**, 136 (1979).

67. C.M. Penney and M. Lapp, *J. Opt. Soc. Am.* **66**, 422 (1976).

68. J.L. Bribes, R. Gaufrès, M. Monan, M. Lapp, and C.M. Penney, *Appl. Phys. Lett.* **28**, 336 (1976).

69. W. Gautschi, *Numerische Mathematik* 3, 381 (1961).

70. P. Bado, P. H. Berens, and K. R. Wilson, in *Picosecond Lasers and Applications*, edited by L. S. Goldberg (Proc. Soc. Photo-Optic. Engin., Bellingham, WA, 1982) Vol. 322, p. 230.

71. P. Bado, P. H. Berens, J. P. Bergsma, S. B. Wilson, K. R. Wilson, and E. J. Heller, in *Picosecond Phenomena III*, edited by K. Eisenthal, R. Hochstrasser, W. Kaiser, and A. Laubereau (Springer-Verlag, Berlin, 1982).

TECHNICAL REPORT DISTRIBUTION LIST, GEN

	No. Copies
Office of Naval Research Attn: Code 472 800 North Quincy Street Arlington, Virginia 22217	2
ONR Western Regional Office Attn: Dr. R. J. Marcus 1030 East Green Street Pasadena, California 91106	1
ONR Eastern Regional Office Attn: Dr. L. H. Peebles Building 114, Section D 666 Summer Street Boston, Massachusetts 02210	1
Director, Naval Research Laboratory Attn: Code 6100 Washington, D.C. 20390	1
The Assistant Secretary of the Navy (RE&S) Department of the Navy Room 4E736, Pentagon Washington, D.C. 20350	1
Commander, Naval Air Systems Command Attn: Code 310C (H. Rosenwasser) Department of the Navy Washington, D.C. 20360	1
Defense Technical Information Center Building 5, Cameron Station Alexandria, Virginia 22314	12
Dr. Fred Saalfeld Chemistry Division, Code 6100 Naval Research Laboratory Washington, D.C. 20375	1
U.S. Army Research Office Attn: CRD-AA-IP P.O. Box 1211 Research Triangle Park, N.C. 27709	1
Naval Ocean Systems Center Attn: Mr. Joe McCartney San Diego, California 92152	1
Naval Weapons Center Attn: Dr. A. B. Amster, Chemistry Division China Lake, California 93555	1
Naval Civil Engineering Laboratory Attn: Dr. R. W. Drisko Port Hueneme, California 93401	1
Department of Physics & Chemistry Naval Postgraduate School Monterey, California 93940	1
Scientific Advisor Commandant of the Marine Corps (Code RD-1) Washington, D.C. 20380	1
Naval Ship Research and Development Center Attn: Dr. G. Bosmajian, Applied Chemistry Division Annapolis, Maryland 21401	1
Naval Ocean Systems Center Attn: Dr. S. Yamamoto, Marine Sciences Division San Diego, California 91232	1
Mr. John Boyle Materials Branch Naval Ship Engineering Center Philadelphia, Pennsylvania 19112	1

TECHNICAL REPORT DISTRIBUTION LIST, GEN

	No. Copies
Mr. James Kelley DTNSRDC Code 2803 Annapolis, Maryland 21402	1
Mr. A. M. Anzalone Administrative Librarian PLASTEC/ARRADCOM Bldg 3401 Dover, New Jersey 07801	1

472:GAN:716:tam
78u472-608

TECHNICAL REPORT DISTRIBUTION LIST, 051A

	No. Copies
~~Dr. M. A. El-Sayed~~ Stet ~~University of California,~~ ~~Los Angeles~~ ~~Department of Chemistry~~ ~~Los Angeles, California 90024~~	1
Dr. M. W. Windsor Washington State University Department of Chemistry Pullman, Washington 99163	1
Dr. E. R. Bernstein Colorado State University Department of Chemistry Fort Collins, Colorado 80521	1
Dr. C. A. Heller Naval Weapons Center Code 6059 China Lake, California 93555	1
Dr. J. R. MacDonald Naval Research Laboratory Chemistry Division Code 6110 Washington, D.C. 20375	1
Dr. G. B. Schuster University of Illinois Chemistry Department Urbana, Illinois 61801	1
Dr. E. M. Eyring University of Utah Department of Chemistry Salt Lake City, Utah 84112	1
Dr. A. Adamson University of Southern California Department of Chemistry Los Angeles, California 90007	1
Dr. M. S. Wrighton Massachusetts Institute of Technology Department of Chemistry Cambridge, Massachusetts 02139	1
Dr. M. Rauhut American Cyanamid Company Chemical Research Division Bound Brook, New Jersey 08805	1
Dr. J. I. Zink University of California, Los Angeles Department of Chemistry Los Angeles, California 90024	1
Dr. B. Schechtman IBM San Jose Research Center 5600 Cottle Road San Jose, California 95143	1
Dr. John Cooper Code 6130 Naval Research Laboratory Washington, D.C. 20375	1

TECHNICAL REPORT DISTRIBUTION LIST, 051B

No. Copies

~~Professor K. Wilson~~
~~Department of Chemistry,~~
~~B-014~~
~~University of California,~~
~~San Diego~~
~~La Jolla, California 92093~~ 1

Professor C. A. Angell
Department of Chemistry
Purdue University
West Lafayette, Indiana 47907 1

Professor P. Meijer
Department of Physics
Catholic University of America
Washington, D.C. 20064 1

Dr. S. Greer
Chemistry Department
University of Maryland
College Park, Maryland 20742 1

Professor P. Delahay
New York University
100 Washington Square East
New York, New York 10003 1

Dr. T. Ashworth
Department of Physics
South Dakota School of
Mines & Technology
Rapid City, South Dakota 57701 1

Dr. G. Gross
New Mexico Institute of
Mining & Technology
Socorro, New Mexico 87801 1

Dr. J. Kassner
Space Science Research Center
University of Missouri - Rolla
Rolla, Missouri 65401 1

Dr. J. Telford
University of Nevada System
Desert Research Institute
Lab of Atmospheric Physics
Reno, Nevada 89507 1

No. Copies

Dr. B. Vonnegut
State University of New York
Earth Sciences Building
1400 Washington Avenue
Albany, New York 12203 1

Dr. Hank Loos
Laguna Research Laboratory
21421 Stans Lane
Laguna Beach, California 92651 1

Dr. John Latham
University of Manchester
Institute of Science & Technology
P.O. Box 88
Manchester, England M601QD 1

TECHNICAL REPORT DISTRIBUTION LIST, 051C

	No. Copies
Dr. M. B. Denton Department of Chemistry University of Arizona Tucson, Arizona 85721	1
Dr. R. A. Osteryoung Department of Chemistry State University of New York at Buffalo Buffalo, New York 14214	1
Dr. B. R. Kowalski Department of Chemistry University of Washington Seattle, Washington 98105	1
Dr. S. P. Perone Department of Chemistry Purdue University Lafayette, Indiana 47907	1
Dr. D. L. Venezky Naval Research Laboratory Code 6130 Washington, D.C. 20375	1
Dr. H. Freiser Department of Chemistry University of Arizona Tuscon, Arizona 85721	
Dr. Fred Saalfeld Naval Research Laboratory Code 6110 Washington, D.C. 20375	1
Dr. H. Chernoff Department of Mathematics Massachusetts Institute of Technology Cambridge, Massachusetts 02139	1
~~Dr. K. Wilson~~ ~~Department of Chemistry~~ University of California, San Diego La Jolla, California	1
Dr. A. Zirino Naval Undersea Center San Diego, California 92132	1
Dr. John Duffin United States Naval Postgraduate School Monterey, California 93940	1
Dr. G. M. Hieftje Department of Chemistry Indiana University Bloomington, Indiana 47401	1
Dr. Victor L. Rehn Naval Weapons Center Code 3813 China Lake, California 93555	1
Dr. Christie G. Enke Michigan State University Department of Chemistry East Lansing, Michigan 48824	1
Dr. Kent Eisentraut, MBT Air Force Materials Laboratory Wright-Patterson AFB, Ohio 45433	1
Walter G. Cox, Code 3632 Naval Underwater Systems Center Building 148 Newport, Rhode Island 02840	1
Professor Isiah M. Warner Texas A&M University Department of Chemistry College Station, Texas 77840	1
Professor George H. Morrison Cornell University Department of Chemisty Ithaca, New York 14853	1
Professor J. Janata Department of Bioengineering University of Utah Salt Lake City, Utah 84112	1
Dr. Carl Heller Naval Weapons Center China Lake, California 93555	1

TECHNICAL REPORT DISTRIBUTION LIST, 051C

	No. Copies
Dr. L. Jarvis Code 6100 Naval Research Laboratory Washington, D.C. 20375	1

END

FILMED